

## Responses to the comments from Reviewer #1

We are very grateful to the reviewer for the positive and careful review. The thoughtful comments have helped improve the manuscript. The reviewer's comments are italicized and our responses immediately follow.

*General Comments: The paper presents an analysis of the impacts of climate change and two ecological factors (CO<sub>2</sub> physiological forcing and land cover change) for the streamflow extremes of the Sanjiangyuan region. The methodology used and the conclusions drawn are sound, and the manuscript is well structured. However, some questions needed to be explained clearly and the English writing of this manuscript needs improvement.*

**Response:** Thanks for the positive comments. We have made extensive modifications to our manuscript for clarification, and have proofread and edited the English carefully. Please see our responses below.

*Lin17 on page 2: '～700' change to '700'*

*Lin40 on page 4: 'Global temperature has been increasing' change to 'Global temperature has increased'*

**Response:** Revised as suggested. (L40 in the revised manuscript)

*Lin 61-62 on page 5: The statement by the authors that 'Thus, it is necessary to assess their combined impacts on the projection of streamflow extremes at different warming levels' is confusing. This sentence needs to be clarified with more evidence to prove the veracity of the statements. In addition, the entire paragraph can be rephrase.*

**Response:** Thanks for the suggestion. The necessity to assess the combined impacts of CO<sub>2</sub> physiological forcing and land cover change is due to their contrary influences on the terrestrial hydrology. We have rephrased the paragraph as follows:

“... In addition to climate change, recent works reveal the importance of the ecological factors (e.g., the CO<sub>2</sub> physiological forcing and land cover change) in modulating the streamflow and its extremes. For example, the increasing CO<sub>2</sub> concentration is found to alleviate the decreasing trend of future streamflow at global scale through decreasing the vegetation transpiration by reducing the stomatal conductance (known as the CO<sub>2</sub> physiological forcing) (Fowler et al., 2019; Wiltshire et al., 2013; Yang et al., 2019; Zhu et al., 2012). Contrary to the CO<sub>2</sub> physiological forcing, the vegetation

greening in a warming climate is found to have a significant role in exacerbating hydrological drought, as it enhances transpiration and dries up the land (Yuan et al., 2018b). However, the relative contributions of CO<sub>2</sub> physiological forcing and vegetation greening to the changes in terrestrial hydrology especially the streamflow extremes are still unknown, and whether their combined impact changes at different warming levels needs to be investigated.” (L51-71)

*Lin 63-66 on page 5: The reasoning behind the choice of the streamflow extremes over the Sanjiangyuan regions needs to be explained.*

**Response:** Thanks for the comment. The reason for the choice of the streamflow extremes over the Sanjiangyuan region is explained from two aspects in the revised manuscript as follows:

- 1) “Hosting the headwaters of the Yellow river, the Yangtze river and the Lancang-Mekong river, the Sanjiangyuan region is known as the “Asian Water Tower” and concerns 700 million people over its downstream areas. Changes in streamflow and its extremes over the Sanjiangyuan region not only influence the local ecosystems, environment and water resources, but also affect the security of food, energy, and water over the downstream areas.” (L72-77)
- 2) “Both the regional climate and ecosystems show significant changes over the Sanjiangyuan region due to global warming (Bibi et al., 2018; Kuang and Jiao, 2016; Liang et al., 2013; Yang et al., 2013; Zhu et al., 2016), which makes it a sound region to investigate the role of climate change and ecological change (e.g., land cover change and CO<sub>2</sub> physiological forcing) in influencing the streamflow and its extremes (Cuo et al., 2014; Ji and Yuan, 2018; Zhu et al., 2013).” (L77-83)

*If historical changes in climate and ecology have significantly altered the terrestrial hydrology over the regions, the terrestrial hydrology also need analysis.*

**Response:** Thanks for the comment. Actually, we have analyzed the terrestrial hydrological changes including the precipitation, evapotranspiration, total runoff and terrestrial water storage at different warming levels in section 3.1 and Figure 4. The results suggest that the regional hydrological cycle is accelerating in a warming climate. Please see the text in the last paragraph in section 3.1.

*At the same time, the characteristics of basin of the headwaters of the Yellow river*

*and Yangtze river should be provided, such as area and discharge.*

**Response:** Thanks for the suggestion. We have added a brief introduction to the characteristics of the study domain in the revised manuscript as follows:

”The Sanjiangyuan region is located at the eastern part of the Tibetan Plateau (Figure 1a), with the total area and mean elevation being  $3.61 \times 10^5$  km<sup>2</sup> and 5000 m respectively. It plays a critical role in providing freshwater, by contributing 35%, 20% and 8% to the total annual streamflow of the Yellow, Yangtze and Lancang-Mekong rivers (Li et al., 2017; Liang et al., 2013). The source regions of Yellow, Yangtze and Lancang-Mekong rivers account for 46%, 44% and 10% of the total area of the Sanjiangyuan individually, and the Yellow river source region has a warmer climate and sparser snow cover than the Yangtze river source region.” (L115-122)

*Lin 67-72 on page 5: Does CO<sub>2</sub> physiological forcing has a significant influence on the terrestrial hydrology and its extremes in Sanjiangyuan or other high-land areas? It would be better to add some related literature.*

**Response:** Thanks for the suggestion. We have added some related literature as suggested: “And the CO<sub>2</sub> physiological forcing is revealed to cause equally large changes in regional flood extremes as the precipitation over the Yangtze and Mekong rivers (Fowler et al., 2019).” (L94-96)

Reference:

Fowler, M. D., Kooperman G. J., Randerson, J. T. and Pritchard M. S.: The effect of plant physiological responses to rising CO<sub>2</sub> on global streamflow, Nat. Clim. Change, 9, 873-879, <https://doi.org/10.1038/s41558-019-0602-x>, 2019.

*Lin 91-94 on page 6: Streamflow observations are daily or monthly streamflow observations? It seem monthly streamflow in this work.*

**Response:** Yes, we used monthly streamflow to evaluate the model. We have clarified it as: “Monthly streamflow observations ..., were used to evaluate the streamflow simulations.” (L123-125)

*Lin 107-109 on page 7: In this study, 11 models in CMIP6 that can reproduce the increased precipitation over the Sanjiangyuan, were chosen for the analysis. Please give more explanation why only precipitation was considered. In addition, can those models correctly simulate the temperature, specific humidity, etc.?*

**Response:** Thanks for the suggestion. We have evaluated the performance of CMIP6 models in representing the trends of other meteorological variables as suggested. Figure R1 shows that the ensemble mean (right panel) and each of the 11 CMIP6 model (left model) chosen in this research can reproduce the sign of historical trends of other meteorological forcings. We have revised the description to avoid misleading information: “... Then, models were chosen for the analysis when the simulated meteorological forcings (e.g., precipitation, temperature, humidity, and shortwave radiation) averaged over the Sanjiangyuan region have the same trend signs as the observations during 1979-2014. Table 1 shows the 11 CMIP6 models that were finally chosen in this study.” (L139-145)

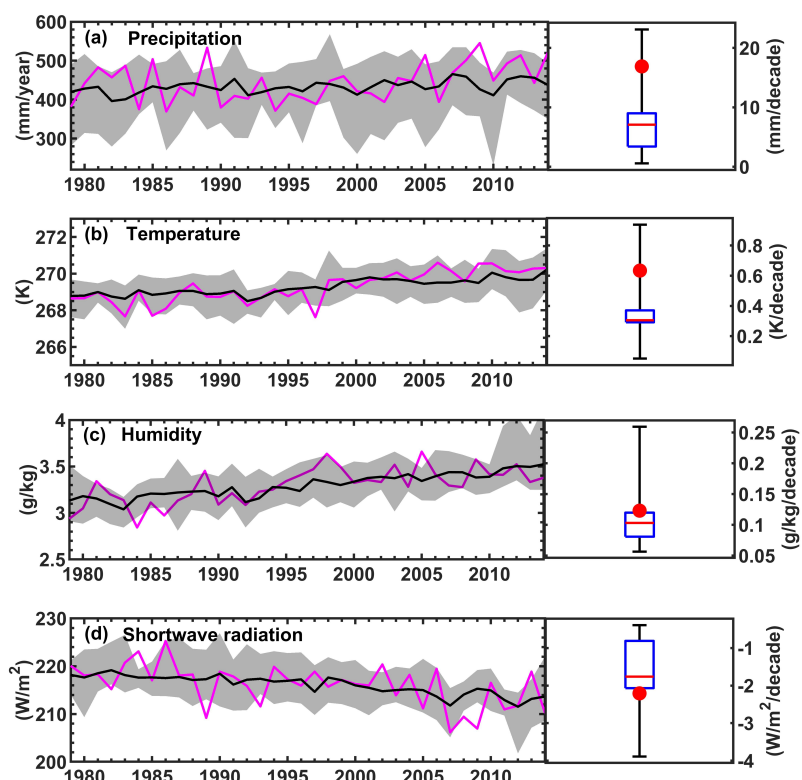


**Figure R1.** (a) Observed (purple line) and CMIP6 model simulated (black line) annual mean precipitation during 1979-2014. Shadings are ranges of all 11 CMIP6 models. The observed precipitation trends during 1979-2014 is shown by red circle on the right panel, while simulated trends of 11 CMIP6 models are shown by the boxplot. (b), (c) and (d) are the same as (a) but for temperature, humidity and shortwave radiation respectively.

*Lin 143-148 on page 7: It is important to show the structure of the model and how it handles the various hydrological processes as mentioned in this part. Maybe you can*

*insert a figure of the structure of the eco-hydrological model.*

**Response:** Thanks for the suggestion. Detailed model introduction and a new Figure 2 have been added in the revised paper as suggested:

“Figure 2 shows the structure and main ecohydrological processes in CSSPv2. The CSSPv2 is rooted in the Common Land Model (CoLM; Dai et al., 2003) with some improvements at hydrological processes. CSSPv2 has a volume-averaged soil moisture transport (VAST) model, which solves the quasi-three dimensional transportation of the soil water and explicitly considers the variability of moisture flux due to subgrid topographic variations (Choi et al., 2007). Moreover, the Variable Infiltration Capacity runoff scheme (Liang et al., 1994), and the influences of soil organic matters on soil hydrological properties were incorporated into the CSSPv2 by Yuan et al. (2018a), to improve its performance in simulating the terrestrial hydrology over the Sanjiangyuan region. Similar to CoLM and Community Land Model (Oleson et al., 2013), vegetation transpiration in CSSPv2 is based on Monin-Obukhov similarity theory, and the transpiration rate is constrained by leaf boundary layer and stomatal conductances. Parameterization of the stomatal conductance ( $g_s$ ) in CSSPv2

is

$$g_s = m \frac{A_n}{P_{CO_2} / P_{atm}} h_s + b \beta_t$$

where the  $m$  is a plant functional type dependent parameter,  $A_n$  is leaf net photosynthesis ( $\mu mol CO_2 m^{-2} s^{-1}$ ),  $P_{CO_2}$  is the CO<sub>2</sub> partial pressure at the leaf surface (Pa),  $P_{atm}$  is the atmospheric pressure (Pa),  $h_s$  is the lead surface humidity,  $b$  is the minimum stomatal conductance ( $\mu mol m^{-2} s^{-1}$ ), while  $\beta_t$  is the soil water stress function. Generally, the stomatal conductance decreases with the increasing of CO<sub>2</sub> concentration. Generally, the stomatal conductance decreases with the increasing of CO<sub>2</sub> concentration.” (L182-207)

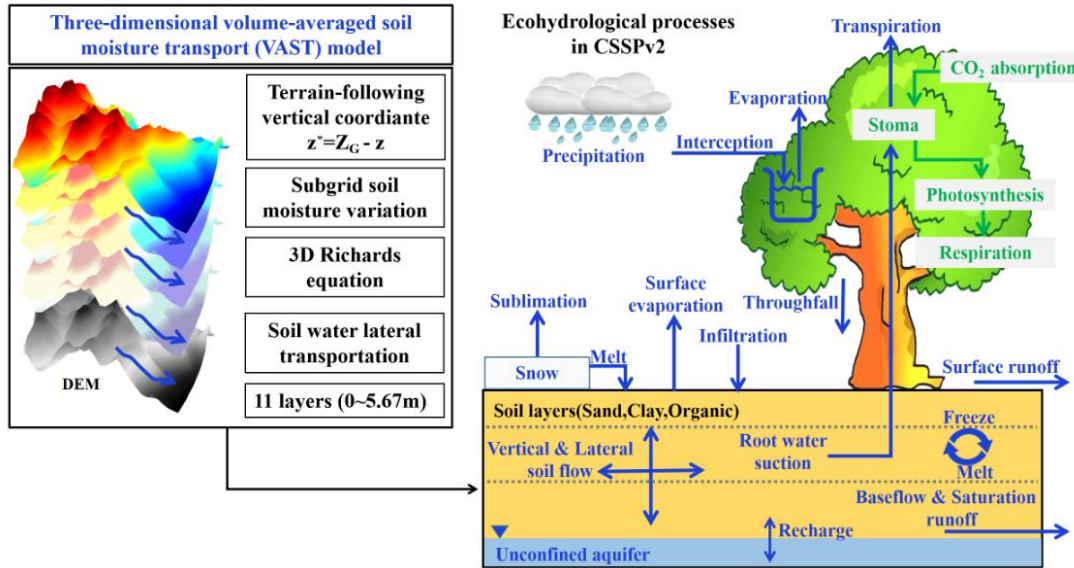


**Figure 2.** Main ecohydrological processes in the Conjunctive Surface-Subsurface Process version 2 (CSSPv2) land surface model.

*Lin 196-198 on page 11: 'the ensemble means of CMIP6 simulations can reproduce the historical increasing trends of temperature, precipitation, and LAI reasonably well.' As shown in the figure 1(d), the ensemble means of CMIP6 seem to hardly simulate the trend of the precipitation. Please give more explanations for this.*

**Response:** Thanks for the suggestion. The previous statement “... reproduce the historical increasing trends of ...” may cause some misunderstanding. We have revised it as: “As shown in Figures 1b-1e, observations (pink lines) show that the annual temperature, precipitation and growing season LAI increase at the rates of 0.63°C/decade ( $p=0$ ), 16.9 mm/decade ( $p=0.02$ ), and 0.02  $m^2/m^2$ /decade ( $p=0.001$ ) during 1979-2014 respectively. The ensemble means of CMIP6 simulations (black lines) can generally capture the historical increasing trends of temperature (0.30 °C/decade,  $p=0$ ), precipitation (7.1 mm/decade,  $p=0$ ) and growing season LAI (0.029  $m^2/m^2$ /decade,  $p=0$ ), although the trends for precipitation and temperature are underestimated.” (L266-273)

*Lin 207-218 on page 11: In this paragraph, the author used different indices to measure the performance of models including Ling-Gupta efficiencies, correlation coefficient, and root mean squared error (RMSE). A simple introduction of those indices can be added in section 2. In addition, the statistical results of the indices in this study can be presented in a table.*

**Response:** Thanks for the suggestion. We have added a brief description of the indices used in the research as: “Correlation coefficient (CC) and root mean squared error (RMSE) were calculated for validating the simulated monthly streamflow, annual evapotranspiration and monthly terrestrial water storage. The King-Gupta efficiency (KGE; Gupta et al., 2009), which is widely used in streamflow evaluations, was also calculated. Above metrics were calculated as follows:

$$CC = \frac{\sum_{i=1}^n (x_i - \bar{x})(y_i - \bar{y})}{\sqrt{\sum_{i=1}^n (x_i - \bar{x})^2 \sum_{i=1}^n (y_i - \bar{y})^2}}$$

$$RMSE = \sqrt{\frac{\sum_{i=1}^n (x_i - y_i)^2}{n}}$$

$$KGE = 1 - \sqrt{(1 - CC)^2 + (1 - \frac{\sigma_x}{\sigma_y})^2 + (1 - \frac{\bar{x}}{\bar{y}})^2}$$

where  $x_i$  and  $y_i$  are observed and simulated variables in a specific month/year  $i$  individually, and  $\bar{x}$  and  $\bar{y}$  are the corresponding monthly/annual means during the evaluation period  $n$ . The  $\sigma_x$  and  $\sigma_y$  are standard deviations for observed and simulated variables, respectively. The KGE ranges from negative infinity to 1, and model simulations can be regarded as satisfactory when the KGE is larger than 0.5 (Moriasi et al., 2007).” (L211-224)

The statistical results of the indices are now shown in Table 3.

**Table 3.** Performance for CSSPv2 model simulations driven by the observed meteorological forcing (CMFD/CSSPv2) and the bias-corrected CMIP6 historical simulations (CMIP6\_His/CSSPv2). The metrics include correlation coefficient (CC), root mean squared error (RMSE), and Kling-Gupta efficiency (KGE). The KGE is only used to evaluate streamflow.

Variables	Experiments	CC	RMSE	KGE
Monthly streamflow at TNH station	CMFD/CSSPv2	0.95	165 m <sup>3</sup> /s	0.94
	CMIP6_His/CSSPv2	0.76	342 m <sup>3</sup> /s	0.71
Monthly streamflow at ZMD	CMFD/CSSPv2	0.93	169 m <sup>3</sup> /s	0.91

station	CMIP6_His/CSSPv2	0.82	257 m <sup>3</sup> /s	0.81
Monthly terrestrial water storage anomaly over the Sanjiangyuan region	CMFD/CSSPv2	0.7	22 mm/month	-
Annual evapotranspiration over the Sanjiangyuan region	CMIP6_His/CSSPv2	0.4	24 mm/month	-
		0.87	14 mm/year	-
		0.47	13 mm/year	-

*Lin 254-255 on page 13: No significant changes? As shown in Figure 4b, the frequency of wet extremes tends to increase by 25%. Please give more explanation.*

**Response:** Thanks for the comment. We have clarified this as: “No statistically significant changes are found ..., as the uncertainty ranges are larger than the ensemble means.” (L332-334)

*Lin 261-264 on page 14: ‘Moreover, the frequency of dry extremes tends to decrease significantly ..’ It seem that the dry extremes over the Yangtze river also need further analysis at different global warming levels. Please clarify.*

**Response:** Thanks for the suggestion. Although the dry extremes over the Yangtze river source region decrease significantly, contributions from the climate change and ecological factors cannot be distinguished due to the small changing magnitude. We have clarified it as:

“Although the frequency of dry extremes also tends to decrease significantly by 35%, 44%, 34% at the three warming levels, the changes are much smaller than those of the wet extremes. Moreover, contributions from climate change and ecological change are both smaller than the uncertainty ranges (not shown), suggesting that their impacts on the changes of dry extremes over the Yangtze river headwater region are not distinguishable. Thus, we mainly focus on the dry extremes over the Yellow river and the wet extremes over the Yangtze river in the following analysis.” (L338-345)

*Lin 298-300 on page 15: Please clarify this sentence.*

**Response:** Thanks for the suggestion. We have revised this sentence and moved it to the front of detailed description of the importance of CO<sub>2</sub> physiological forcing and land cover change:

“Although the contribution from climate change (red bars in Figures 7a-7b) is greater than the ecological factors (blue and cyan bars in Figures 7a-7b), influences of CO<sub>2</sub>

physiological forcing and land cover change are nontrivial. ... Over the Yellow river, the combined impact of the two ecological factors ... reduces the increasing trend of dry extremes caused by climate change (red bars) by 18~22% at 1.5 and 2.0 °C warming levels, while intensifies the dry extremes by 9% at 3.0°C warming level. ... Over the Yangtze river, ... increases the wet extremes by 9% at 1.5°C warming level while decreases the wet extremes by 12% at 3.0°C warming level.” (L371-385)

*Lin 321-323 on page 11: A section on uncertainties should be included. Climate model and eco-hydrological model are sources of uncertainties. For example, according to Fig 2, the simulations tend to underestimate the high flow, which will inevitably affect the results.*

**Response:** Thanks for the suggestion. We do agree with the reviewer that both global climate models (GCMs) and hydrological models are sources of uncertainties. Actually, we have used the bootstrap method to estimate the uncertainty caused by GCMs. We have added detailed information for the uncertainty estimations as follows:

“The relative changes in frequency of dry/wet extremes between the reference period and different warming periods were first calculated for each GCM under each SSP scenario, and the ensemble means were then determined for each warming level. To quantify the uncertainty, the above calculations were repeated by using the bootstrap 10,000 times, and 11 GCMs were resampled with replacement during each bootstrap (Christopher et al., 2018). The 5% and 95% percentiles of the total 10,000 estimations were finally taken as the 5~95% uncertainty ranges.” (L257-263)

We do not add a new section to discuss the uncertainties, because analysis of uncertainties that caused by GCMs is already included in the results and only the robust changes are taken into consideration in this research.

“However, the dry extreme frequency will further increase to 77% and 125% at the 2.0 and 3.0°C warming levels and the results become significant (Figure 5b).”(L329-332).

“No statistically significant changes are found for the wet extremes at all warming levels over the Yellow River headwater region, as the uncertainty ranges are larger than the ensemble means.”(L332-334)

However, we have added some discussions on the uncertainties caused by land surface hydrological model, as only one land surface model was used in this work. “Although we used 11 CMIP6 models combined with two SSP scenarios to reduce the uncertainty of future projections caused by GCMs, using a single land surface model may result in uncertainties (Marx et al., 2018). However, considering the good performance of the CSSPv2 land surface model over the Sanjiangyuan region and the dominant role of GCMs’ uncertainty (Zhao et al., 2019; Samaniego et al., 2017), uncertainty from the CSSPv2 model should have limited influence on the robust of the result.” (L447-453)

*Figure 1.(d) ‘growthing season leaf area index’, while Line 483 ‘growing season leaf area index’?*

**Response:** We have corrected the ‘growthing season leaf area index’ as ‘growing season leaf area index’ in the revised Figure 1.

*Figure 4.(1) ‘Simulated monthly streamflow climatology’ change ‘Simulated monthly streamflow’*

**Response:** Revised as suggested.

## Responses to the comments from Reviewer #2

We are very grateful to the reviewer for the positive and careful review. The thoughtful comments have helped improve the manuscript. The reviewer's comments are italicized and our responses immediately follow.

*This is an interesting paper that analyzes the future changes in the streamflow extremes and its contributions from ecological factors over the Sanjiangyuan region based on observational data and model outputs driven by the CMIP6 data. Besides a regional accelerated hydrological cycle at different warming levels, the high risk of dry and wet extremes over the headwater of Yellow river and Yangtze river are also found. More importantly, the individual and combined impacts of land cover change and CO<sub>2</sub> physiological forcing on projected hydrological changes are figured out and emphasized. Overall, the manuscript is well structured and presented, and there are a few minor comments below.*

**Response:** Thanks for the comment.

1. *Line 156: I suggest references for CLM and CoLM are required here.*

**Response:** Revised as suggested.

2. *Lines 242-243: How to understand the phenomena that both the ET and runoff increase with the increase in precipitation, while the local water storage TWS changes little? Is it a common issue in the accelerated hydrological cycle in other regions? Maybe a further explanation for the little TWS change would be useful.*

**Response:** Thanks for the suggestion. We have explained it as follows:

“The terrestrial water storage, however, shows a slight but significant decreasing trend as increased evapotranspiration and runoff are larger than the increased precipitation. This decreasing trend of terrestrial water storage in the warming future is also found in six major basins in China (Jia et al., 2020).” (L410-414)

3. *Line 251: Is "55%" statistically significant? I also suggest the significance tests for the rest of the changes at different warming levels in sections 3.2 and 3.3.*

**Response:** Thanks for the suggestion. We have clarified it as:

“The frequency of streamflow dry extremes over the Yellow river is found to increase by 55% at 1.5°C warming level (Figure 5b), but the uncertainty is larger than the

ensemble mean.” (L327-329)

Actually, we used the bootstrap method to estimate the uncertainty, and changes are considered to be significant when the ensemble mean is larger than the uncertainty range. We have clarified as:

“The relative changes in frequency of dry/wet extremes between the reference period and different warming periods were first calculated for each GCM under each SSP scenario, and the ensemble means were then determined for each warming level. To quantify the uncertainty, the above calculations were repeated by using the bootstrap 10,000 times, and 11 GCMs were resampled with replacement during each bootstrap (Christopher et al., 2018). The 5% and 95% percentiles of the total 10,000 estimations were finally taken as the 5~95% uncertainty ranges.” (L257-263)

We have also added some statements on the uncertainties or significance in sections 3.2 and 3.3 as suggested:

“... the results become significant (Figure 5b). No statistically significant changes are found ..., as the uncertainty ranges are larger than the ensemble means.”(L332-334)

“Moreover, contributions from climate change and ecological change are both smaller than the uncertainty ranges (not shown), suggesting that their impacts on the changes of dry extremes over the Yangtze river headwater region are not distinguishable.” (L340-343)

4. *Line 270: In Figure 5a, the PDF of precipitation at 1.5 degrees warming level doesn't shift to the right against the reference period. Please correct the statement.*

**Response:** We have revised it as: “Over the Yellow river, PDFs of precipitation and evapotranspiration both shift to the right against the reference period, except for the precipitation at 1.5°C warming level.” (L350-352)

5. *Lines 269-272 and Lines 281-282: “Over the Yellow river. . . the increasing trend of ET is stronger than that of precipitation”. “Over the Yangtze river, however, intensified ET is much smaller than the increased precipitation”. How to understand the opposite phenomenon over the two regions? The change in ET significantly influences the streamflow extremes changes over the Yellow and Yangtze rivers headwaters. Maybe a brief mention of that here would be useful.*

**Response:** Thanks for the comment. Actually, differences between headwaters of Yellow and Yangtze rivers are mainly caused by precipitation changes, as the increasing rate of ET at the Yangtze river headwater are similar to that at the Yellow river headwater. We have revised the statement as: “Over the Yangtze river, however, intensified precipitation is much larger than the increased evapotranspiration,...”. (L365-366)

Different changing rates of precipitation over these two river source regions are beyond this work, so we do not discuss this in detail. Further work is needed to investigate the changes in horizontal moisture transport and local land-atmospheric exchanges.

6. *Line 278: Change “Figure 3e” to “Figure 5e”?*

**Response:** Thanks. We have changed “Figure 3e” to “Figure 6e” as a new figure was added to show the model structure.

7. *Lines 274-280: “The above two factors together induce a heavier left tail in the PDFs of P-ET for the warming future than the reference period (Figure 5e). This indicates a higher probability of less water left for runoff generation at different warming levels, given little changes in TWS (section 3.1). Moreover, Figure 3e also shows little change to the right tails in the PDF of P-ET ( $P-ET > 130mm$ ) at different warming levels, suggesting little change to the probability of high residual water.” It’s hard to clearly distinguish the “heavier left tail” and “little change to the right tails” in Figure 5e and thus explain the large dry extremes and insignificant wet extremes. Can you give a more clear clue for that?*

**Response:** Thanks for the suggestion. We have calculated the cumulative probability for both low and high P-ET values and added them in the manuscript to show the changes of PDFs more clearly.

“... together induce a heavier left tail in the PDF of P-ET .... The probability of  $P-ET < 80mm$  increases from 0.1 during historical period to 0.11, 0.13 and 0.16 at 1.5, 2.0 and 3.0°C warming levels individually. ... shows little change to the right tails in the PDF of P-ET as probability for  $P-ET > 130mm$  stays around 0.1 at different warming levels ...” (L357-362)

8. *Line 320: How to get the value of “4-6%” for the acceleration of the hydrological*

*cycle under global warming of 1.5 degrees?*

**Response:** Thanks for the comment. We have clarified as: "... is found to accelerate by 4~6% ..., according to the relative changes of precipitation, evapotranspiration and total runoff." (L409-410)

*9. Lines 323-324: What's the period for the change of streamflow extremes?*

**Response:** We have clarified as "Although ... compared with that during 1985~2014." (L416-417)

*10. Lines 327-329: I'm not sure what does the "nonlinear changes" mean. Can you add some detail for the nonlinear changes from future warming over Europe?*

**Response:** We have clarified the nonlinear changes as "The changes from 1.5 to 2.0 and 3.0°C are nonlinear compared with that from reference period to 1.5°C, ..." (L420-422)

To be specific, the wet extremes over Yangtze river source region increase by 138% at 1.5°C warming levels, which indicates a linear rate of 46%/0.5°C. However, projected change of wet extremes from 1.5 to 2.0°C warming levels is 64% which is much larger than the linear rate.

*11. Lines 347-350: "Considering the LAI projections from different CMIP6 models are induced by the climate change, it can be inferred that the indirect influence of climate change (e.g., through land cover change) has the same and even larger importance. . . compared with the direct influence (e.g., through precipitation and evapotranspiration)." How to understand the direct and indirect influence of climate change on the streamflow extremes changes? Can you give a further explanation for that?*

**Response:** The indirect influence of climate change means the climate change will induce land cover change and then the land cover change can also influence the hydrological extremes. The direct influence of climate change means the influence of meteorological forcings (e.g., precipitation, temperature, radiation) changes.

1   **Accelerated hydrological cycle over the Sanjiangyuan region induces**  
2   **more streamflow extremes at different global warming levels**

3

4                   Peng Ji<sup>1,2</sup>, Xing Yuan<sup>3</sup>, Feng Ma<sup>3</sup>, Ming Pan<sup>4</sup>

5

6   <sup>1</sup>Key Laboratory of Regional Climate-Environment for Temperate East Asia, Institute  
7   of Atmospheric Physics, Chinese Academy of Sciences, Beijing 100029, China

8   <sup>2</sup>College of Earth and Planetary Sciences, University of Chinese Academy of Sciences,  
9   Beijing 1000493, China

10   <sup>3</sup>School of Hydrology and Water Resources, Nanjing University of Information  
11   Science and Technology, Nanjing 210044, China

12   <sup>4</sup>Department of Civil and Environmental Engineering, Princeton University, Princeton,  
13   New Jersey, USA

14

15   *Correspondence to:* Xing Yuan (xyuan@nuist.edu.cn)

16 **Abstract.** Serving source water for the Yellow, Yangtze and Lancang-Mekong rivers,  
17 the Sanjiangyuan region concerns  $\sim$ 700 million people over its downstream areas.  
18 Recent research suggests that the Sanjiangyuan region will become wetter in a  
19 warming future, but future changes in streamflow extremes remain unclear due to the  
20 complex hydrological processes over high-land areas and limited knowledge of the  
21 influences of land cover change and CO<sub>2</sub> physiological forcing. Based on high  
22 resolution land surface modeling during 1979~2100 driven by the climate and  
23 ecological projections from 11 newly released Coupled Model Intercomparison  
24 Project Phase 6 (CMIP6) climate models, we show that different accelerating rates of  
25 precipitation and evapotranspiration at 1.5°C global warming level induce 55% more  
26 dry extremes over Yellow river and 138% more wet extremes over Yangtze river  
27 headwaters compared with the reference period (1985~2014). An additional 0.5°C  
28 warming leads to a further nonlinear and more significant increase for both dry  
29 extremes over Yellow river (22%) and wet extremes over Yangtze river (64%). The  
30 combined role of CO<sub>2</sub> physiological forcing and vegetation greening, which used to  
31 be neglected in hydrological projections, is found to alleviate dry extremes at 1.5 and  
32 2.0°C warming levels but to intensify dry extremes at 3.0°C warming level. Moreover,  
33 vegetation greening contributes half of the differences between 1.5 and 3.0°C  
34 warming levels. This study emphasizes the importance of ecological processes in  
35 determining future changes in streamflow extremes, and suggests a “dry gets drier,  
36 wet gets wetter” condition over headwaters.

37 **Keywords** Terrestrial hydrological cycle, streamflow extremes, global warming levels,



39     1 Introduction

40     Global temperature has ~~been~~ increasing at a rate of 1.7°C/decade since 1970,  
41     contrary to the cooling trend over the past 8000 years (Marcott et al., 2013). The  
42     temperature measurements suggest that 2015-2019 is the warmest five years and  
43     2010-2019 is also the warmest decade since 1850 (WMO, 2020). To mitigate the  
44     impact of this unprecedented warming on the global environment and human society,  
45     195 nations adopted the Paris Agreement which decides to “hold the increase in the  
46     global average temperature to well below 2°C above pre-industrial levels and pursuing  
47     efforts to limit the temperature increase to 1.5°C”.

48     The response of regional and global terrestrial hydrological processes, including  
49     streamflow and its extremes, to different global warming levels has been investigated  
50     by numerous studies in recent years (Chen et al., 2017; Döll et al., 2018; Marx et al.,  
51     2018; Mohammed et al., 2017; Thober et al., 2018; Zhang et al., 2016). In addition to  
52     climate change, recent works reveal the importance of ~~However, the ecological factors~~  
53     (e.g., the CO<sub>2</sub> physiological forcing and land cover change) in modulating the  
54     streamflow and its extremes~~whose importance in modulating the terrestrial~~  
55     hydrological responses is emphasized by recent research,~~are often unaccounted for~~  
56     in studies regarding the changes in hydrological extremes. For example, the  
57     increasing CO<sub>2</sub> concentration is found to alleviate the decreasing trend of future  
58     streamflow at global scale through decreasing the vegetation transpiration by reducing  
59     the stomatal conductance (known as the CO<sub>2</sub> physiological forcing) (Fowler et al.,  
60     2019; Wiltshire et al., 2013; Yang et al., 2019; Zhu et al., 2012). ~~the suppression of~~

61 ~~stomatal conductance (thus vegetation transpiration) by increased CO<sub>2</sub> concentration~~  
62 ~~(known as the CO<sub>2</sub> physiological forcing), is found to alleviate the decreasing trend of~~  
63 ~~streamflow in the future at global scale (Wiltshire et al., 2013; Yang et al., 2019; Zhu~~  
64 ~~et al., 2012). While~~Contrary to the CO<sub>2</sub> physiological forcing, the vegetation greening  
65 in a warming climate is found to have a significant role ~~in~~ in exacerbating hydrological  
66 drought, as it enhances transpiration and dries up the land (Yuan et al., 2018b).  
67 However, the relative contributions of CO<sub>2</sub> physiological forcing and vegetation  
68 greening to the changes in terrestrial hydrology especially the streamflow extremes  
69 are still unknown, and whether~~Thus, it is necessary to assess~~ their combined impacts  
70 ~~on the projection of streamflow extremes changes~~ at different warming levels needs to  
71 be investigated.

72 Hosting the headwaters of the Yellow river, the Yangtze river and the  
73 Lancang-Mekong river, the Sanjiangyuan region is ~~also~~-known as the “Asian Water  
74 Tower” and concerns 700 million people over its downstream areas. Changes in  
75 streamflow and its extremes over the Sanjiangyuan region not only influence the local  
76 ecosystems, environment and water resources, but also affect the security of food,  
77 energy, and water over the downstream areas. Both the regional climate and  
78 ecosystems show significant changes over the Sanjiangyuan region due to global  
79 warming (Bibi et al., 2018; Kuang and Jiao, 2016; Liang et al., 2013; Yang et al., 2013;  
80 Zhu et al., 2016), which makes it a sound region to investigate the role of climate  
81 change and ecological change (e.g., land cover change and CO<sub>2</sub> physiological forcing)  
82 in influencing the streamflow and its extremes (Cuo et al., 2014; Ji and Yuan, 2018;

83 Zhu et al., 2013). The global warming has induced significant changes in the  
84 regionalalpine climate and fragile ecosystem over make the Sanjiangyuan region  
85 sensitive to the global warming (Kuang and Jiao, 2016; Liang et al., 2013; Sadia et  
86 al., 2018; Yang et al., 2013; Zhu et al., 2016), which then alters the regional  
87 streamflow and its extremes (Cuo et al., 2014; Ji and Yuan, 2018; Fowler et al., 2019;  
88 Zhu et al., 2013). For example, Historical changes in climate and ecology (e.g. land  
89 cover) have significantly altered the terrestrial hydrology and its extremes (Ji and  
90 Yuan, 2018; Yuan et al., 2018a). For example, the Yellow river headwater region,  
91 which provides more than one third of the total streamflow in the Yellow river,  
92 experienceare found to cause significant reduction in mean and high flows during  
93 1979-2005, which potentially increasesing drought risk over its downstream areas (Ji  
94 and Yuan, 2018). And the CO<sub>2</sub> physiological forcing is revealed to cause equally large  
95 changes in regional flood extremes as the precipitation over the Yangtze and Mekong  
96 rivers (Fowler et al., 2019). Recent research suggests that the Sanjiangyuan region  
97 will become warmer and wetter in the future, and extreme precipitation will also  
98 increase at the 1.5°C global warming level and further intensify with a 0.5°C  
99 additional warming (Li et al., 2018; Zhao et al., 2019). However, how the streamflow  
100 extremes would respond to the 1.5°C warming, what an additional 0.5°C or even  
101 greater warming would cause, and how much contributions do the ecological factors  
102 (e.g., CO<sub>2</sub> physiological forcing and land cover change) have, are still unknown. This  
103 makes it difficult to assess the climate and ecological impact on this vital headwaters  
104 region.

105 In this study, we investigate the future changes in the streamflow extremes over  
106 the Sanjiangyuan region from an integrated eco-hydrological perspective by taking  
107 CO<sub>2</sub> physiological forcing and land cover change into consideration. The combined  
108 impacts of the above two ecological factors at different global warming levels are also  
109 quantified and compared with the impact of climate change. The results will help  
110 understand the role of ecological factors in future terrestrial hydrological changes  
111 over the headwater regions like the Sanjiangyuan, and provide guidance and support  
112 for the stakeholders to make relevant decisions and plans.

113 **2 Data and methods**

114 **2.1 Study domain and Observational Data**

115 The Sanjiangyuan region is located at the eastern part of the Tibetan Plateau  
116 (Figure 1a), with the total area and mean elevation being  $3.61 \times 10^5 \text{ km}^2$  and 5000 m  
117 respectively. It plays a critical role in providing freshwater, by contributing 35%, 20%  
118 and 8% to the total annual streamflow of the Yellow, Yangtze and Lancang-Mekong  
119 rivers (Li et al., 2017; Liang et al., 2013). The source regions of Yellow, Yangtze and  
120 Lancang-Mekong rivers account for 46%, 44% and 10% of the total area of the  
121 Sanjiangyuan individually, and the Yellow river source region has a warmer climate  
122 and sparser snow cover than the Yangtze river source region.

123 Monthly Streamflow observations from the Tangnaihai (TNH) and the  
124 Zhimenda (ZMD) hydrological stations (Figure 1a), which were provided by the local  
125 authorities, were used to evaluate the streamflow simulations. Data periods are  
126 1979-2011 and 1980-2008 for the Tangnaihai and Zhimenda stations individually.

127 Monthly terrestrial water storage change observation and its uncertainty during  
128 2003-2014 was provided by the Jet Propulsion Laboratory (JPL), which used the mass  
129 concentration blocks (mascons) basis functions to fit the Gravity Recovery and  
130 Climate Experiment (GRACE) satellite's inter-satellite ranging observations (Watkins  
131 et al., 2015). The Model Tree Ensemble evapotranspiration (MTE\_ET; Jung et al.,  
132 2009) and the Global Land Evaporation Amsterdam Model evapotranspiration  
133 (GLEAM\_ET) version 3.3a (Martens et al., 2017) were also used to evaluate the  
134 model performance on ET simulation.

135 **2.2 CMIP6 Data**

136 Here, 19 Coupled Model Intercomparison Project phase 6 (CMIP6, Eyring et al.,  
137 2016) models which provide precipitation, near-surface temperature, specific  
138 humidity, 10-m wind speed, surface downward shortwave and longwave radiations at  
139 daily timescale were first selected for evaluation. Then, models11-of-them were  
140 chosen for the analysis when the simulatedas— meteorological forcings (e.g.,  
141 precipitation, temperature, humidity, and shortwave radiation) averaged over the  
142 Sanjiangyuan region they have the same trend signs as the observations during  
143 1979-2014. Table 1 shows the 11 CMIP6 models that were finally chosen in this  
144 study an best reproduce the increasing precipitation over the Sanjiangyuan region  
145 during 1979-2014 (Table 1). For the future projection (2015-2100), we chose two  
146 Shared Socioeconomic Pathways (SSP) experiments: SSP585 and SSP245. SSP585  
147 combines the fossil-fueled development socioeconomic pathway and 8.5W/m<sup>2</sup> forcing  
148 pathway (RCP8.5), while SSP245 combines the moderate development

149 socioeconomic pathway and 4.5 W/m<sup>2</sup> forcing pathway (RCP4.5) (O'Neill et al.,  
150 2016). Land cover change is quantified by leaf area index (LAI) as there is no  
151 significant transition between different vegetation types (not shown) according to the  
152 Land-use Harmonization 2 (LUH2) dataset  
153 (<https://esgf-node.llnl.gov/search/input4mips/>). For the CNRM-CM6-1, FGOALS-g3  
154 and CESM2, the ensemble mean of LAI simulations from the other 8 CMIP6 models  
155 was used because CNRM-CM6-1 and FGOALS-g3 do not provide dynamic LAI  
156 while the CESM2 simulates an abnormally large LAI over the Sanjiangyuan region.  
157 To avoid systematic bias in meteorological forcing, the trend-preserved bias  
158 correction method suggested by ISI-MIP (Hempel et al., 2013), was applied to the  
159 CMIP6 model simulations at monthly scale. The China Meteorological Forcing  
160 Dataset (CMFD) is taken as meteorological observation (He et al., 2020). For each  
161 month, temperature bias in CMIP6 simulations during 1979-2014 was directly  
162 deducted. Future temperature simulations in SSP245 and SSP585 experiments were  
163 also adjusted according to the historical bias. Other variables were corrected by using  
164 a multiplicative factor, which was calculated by using observations to divide  
165 simulation during 1979-2014. In addition, monthly leaf area index was also adjusted  
166 to be consistent with satellite observation using the same method as temperature. All  
167 variables were first interpolated to the 10 km resolution over the Sanjiangyuan region  
168 and the bias correction was performed for each CMIP6 model at each grid. After bias  
169 correction, absolute changes of temperature and leaf area index, and relative changes  
170 of other variables were preserved at monthly time scale (Hempel et al., 2013). Then,

171 the adjusted CMIP6 daily meteorological forcings were disaggregated into hourly  
172 using the diurnal cycle ratios from the China Meteorological Forcing Dataset (CMFD;  
173 He et al., 2020).

174 The historical CO<sub>2</sub> concentration used here is the same as the CMIP6 historical  
175 experiment (Meinshausen et al., 2017), while future CO<sub>2</sub> concentration in SSP245 and  
176 SSP585 scenarios came from simulations of a reduced-complexity carbon-cycle  
177 model MAGICC7.0 (Meinshausen et al., 2020)<http://greenhousegases.science.unimelb.edu.au/>.

### 179 **2.3 Experimental design**

180 The land surface model used in this study is the Conjunctive Surface-Subsurface  
181 Process model version 2 (CSSPv2), which has been proved to simulate the energy and  
182 water processes over the Sanjiangyuan region well (Yuan et al., 2018a). Figure 2  
183 shows the structure and main ecohydrological processes in CSSPv2. The CSSPv2 is  
184 rooted in the Common Land Model (CoLM; Dai et al., 2003) with some  
185 improvements at hydrological processes. CSSPv2 has a volume-averaged soil  
186 moisture transport (VAST) model, which solves the quasi-three dimensional  
187 transportation of the soil water and explicitly considers the variability of moisture flux  
188 due to subgrid topographic variations (Choi et al., 2007). Moreover, the Variable  
189 Infiltration Capacity runoff scheme (Liang et al., 1994), and the influences of soil  
190 organic matters on soil hydrological properties were incorporated into the CSSPv2 by  
191 Yuan et al. (2018a), to improve its performance in simulating the terrestrial hydrology  
192 over the Sanjiangyuan region., incorporates the variable infiltration capacity runoff

193 scheme, and considers hydrological influences of soil organic matters. Similar to  
194 CoLM and Community Land Model (Oleson et al., 2013), vegetation transpiration in  
195 CSSPv2 is based on Monin-Obukhov similarity theory, and the transpiration rate is  
196 constrained by leaf boundary layer and stomatal conductances. Systematic evaluation  
197 has proved that CSSPv2 well simulates the energy and water processes over the  
198 Sanjiangyuan region (Yuan et al., 2018a). Parameterization of the stomatal  
199 conductance ( $g_s$ ) in CSSPv2 is

200

$$g_s = m \frac{A_n}{P_{CO_2} / P_{atm}} h_s + b \beta_t$$

201 where the  $m$  is a plant functional type dependent parameter,  $A_n$  is leaf net  
202 photosynthesis ( $\mu mol CO_2 m^{-2} s^{-1}$ ),  $P_{CO_2}$  is the CO<sub>2</sub> partial pressure at the leaf  
203 surface (Pa),  $P_{atm}$  is the atmospheric pressure (Pa),  $h_s$  is the lead surface  
204 humidity,  $b$  is the minimum stomatal conductance ( $\mu mol m^{-2} s^{-1}$ ), while  $\beta_t$  is the  
205 soil water stress function. This parameterization is also used in the Community Land  
206 Surface Model (CLM) and the Common Land Surface Model (CoLM). Generally, the  
207 stomatal conductance decreases with the increasing of CO<sub>2</sub> concentration.

208 First, bias-corrected meteorological forcings from CMIP6 historical experiment  
209 were used to drive the CSSPv2 model (CMIP6\_His/CSSPv2). All simulations were  
210 conducted for two cycles during 1979-2014 at half-hourly time step and 10 km spatial  
211 resolution, with the first cycle serving as the spin-up. Correlation coefficient (CC) and  
212 root mean squared error (RMSE) were calculated for validating the simulated monthly  
213 streamflow, annual evapotranspiration and monthly terrestrial water storage. The  
214 King-Gupta efficiency (KGE; Gupta et al., 2009), which is widely used in streamflow

215 evaluations, was also calculated. Above metrics were calculated as follows:

$$216 \quad CC = \frac{\sum_{i=1}^n (x_i - \bar{x})(y_i - \bar{y})}{\sqrt{\sum_{i=1}^n (x_i - \bar{x})^2 \sum_{i=1}^n (y_i - \bar{y})^2}}$$

$$217 \quad RMSE = \sqrt{\frac{\sum_{i=1}^n (x_i - y_i)^2}{n}}$$

$$218 \quad KGE = 1 - \sqrt{(1 - CC)^2 + (1 - \frac{\sigma_x}{\sigma_y})^2 + (1 - \frac{\bar{x}}{\bar{y}})^2}$$

219 where  $x_i$  and  $y_i$  are observed and simulated variables in a specific month/year  $i$   
220 individually, and  $\bar{x}$  and  $\bar{y}$  are the corresponding monthly/annual means during the  
221 evaluation period  $n$ . The  $\sigma_x$  and  $\sigma_y$  are standard deviations for observed and  
222 simulated variables, respectively. The KGE ranges from negative infinity to 1, and  
223 model simulations can be regard as satisfactory when the KGE is larger than 0.5  
224 (Moriasi et al., 2007).

225 Second, bias-corrected meteorological forcings in SSP245 and SSP585 were  
226 used to drive CSSPv2 during 2015-2100 with dynamic LAI and CO<sub>2</sub> concentration  
227 (CMIP6\_SSP/CSSPv2). Initial conditions of CMIP6\_SSP/CSSPv2 came from the last  
228 year in CMIP6\_His/CSSPv2.

229 Then, the second step was repeated twice by fixing the monthly LAI  
230 (CMIP6\_SSP/CSSPv2\_FixLAI) and mean CO<sub>2</sub> concentration  
231 (CMIP6\_SSP/CSSPv2\_FixCO2) at 2014 level. The difference between  
232 CMIP6\_SSP/CSSPv2 and CMIP6\_SSP/CSSPv2\_FixLAI is regarded as the net effect  
233 of land cover change, and the difference between CMIP6\_SSP/CSSPv2 and

234 CMIP6\_SSP/CSSPv2\_FixCO2 is regarded as the net effect of CO<sub>2</sub> physiological  
235 forcing.

236 **2.4 Warming level determination**

237 A widely used time-sampling method was adopted to determine the periods of  
238 different global warming levels (Chen et al., 2017; Döll et al., 2018; Marx et al., 2018;  
239 Mohammed et al., 2017; Thober et al., 2018). According to the HadCRUT4 dataset  
240 (Morice et al., 2012), the global mean surface temperature has increased by 0.66°C  
241 from the pre-industrial era (1850-1900) to the reference period defined as 1985-2014.  
242 Then, starting from 2015, 30-years running mean global temperatures were compared  
243 to those of the 1985-2014 period for each GCM simulation. And the  
244 1.5°C/2.0°C/3.0°C warming period is defined as the 30-years period when the  
245 0.84°C/1.34°C/2.34°C global warming, compared with the reference period  
246 (1985-2014), is first reached. The median years of identified 30-year periods, referred  
247 as “crossing years”, are shown in Table 2.

248 **2.5 Definition of dry and wet extremes and robustness assessment**

249 In this research, the standardized streamflow index (SSI) was used to define dry  
250 and wet extremes (Vicente-Serrano et al., 2012; Yuan et al., 2017). A gamma  
251 distribution was first fitted using July-September (flood season) mean streamflow  
252 during the reference period. Then the fitted distribution was used to calculate the  
253 standardized deviation of the July-September mean streamflow (i.e. SSI) in each year  
254 during both the reference and projection periods. Here, dry and wet extremes were  
255 defined as where SSIs are smaller than -1.28 (a probability of 10%) and larger than

256 1.28 respectively.

257 The relative changes in frequency of dry/wet extremes between the reference  
258 period and different warming periods were first calculated for each GCM under each  
259 SSP scenario, and the ensemble means were then determined for each warming level.  
260 To quantify the uncertainty, the above calculations were repeated by using the  
261 bootstrap 10,000 times, and 11 GCMs were resampled with replacement during each  
262 bootstrap (Christopher et al., 2018). The 5% and 95% percentiles of the total 10,000  
263 estimations were finally taken as the 5~95% uncertainty ranges.

### 264 3 Results

#### 265 3.1 Terrestrial hydrological changes at different warming levels

266 As shown in Figures 1b-1e, observations (pink lines) show that the annual  
267 temperature, precipitation and growing season LAI increase at the rates of  
268 0.63°C/decade (p=0), 16.9 mm/decade (p=0.02), and 0.02 m<sup>2</sup>/m<sup>2</sup>/decade (p=0.001)  
269 during 1979-2014 respectively. The ensemble means of CMIP6 simulations (black  
270 lines) can generally capture the historical increasing trends of temperature

271 (0.30 °C/decade, p=0), precipitation (7.1 mm/decade, p=0) and growing season LAI

272 (0.029 m<sup>2</sup>/m<sup>2</sup>/decade, p=0), although the trends for precipitation and temperature are

273 underestimated. for growing season LAI (pink lines) reasonably well. In 2015-2100,

274 the SSP245 scenario (blue lines) shows continued warming, wetting and greening

275 trends, and the trends are larger in the SSP585 scenario (red lines). The CO<sub>2</sub>

276 concentration also keeps increasing during 2015-2100 and reaches to 600 ppm and

277 1150 ppm in 2100 for the SSP245 and SSP585 scenarios respectively. Although the

278 SSP585 scenario reaches the same warming levels earlier than the SSP245 scenario  
279 (Table 2), there is no significant difference between them in the meteorological  
280 variables during the same warming period (not shown). Thus, we do not distinguish  
281 SSP245 and SSP585 scenarios at the same warming level in the following analysis.

282 Figure 23 and Table 3 shows the evaluation of model simulation. Driven by  
283 observed meteorological and ecological forcings, the CMFD/CSSPv2 simulates  
284 monthly streamflow over the Yellow and Yangtze river headwaters quite well.  
285 Compared with the observation at Tangnaihai (TNH) and Zhimenda (ZMD) stations,  
286 the Kling-Gupta efficiencies of the CMFD/CSSPv2 simulated monthly streamflow are  
287 0.94 and 0.91 respectively. The simulated monthly Terrestrial Water Storage Anomaly  
288 (TWSA) during 2003-2014 in CMFD/CSSPv2 also agrees with the GRACE satellite  
289 observation and captures the increasing trend. For the interannual variations of  
290 evapotranspiration, CMFD/CSSPv2 is consistent with the ensemble mean of the  
291 GLEAM\_ET and MTE\_ET products, and the correlation coefficient and root mean  
292 squared error (RMSE) during 1982-2011 are 0.87 ( $p<0.01$ ) and 14 mm/year  
293 respectively. This suggests the good performance of the CSSPv2 in simulating the  
294 hydrological processes over the Sanjiangyuan region. Although meteorological and  
295 ecological outputs from CMIP6 models have coarse resolutions ( $\sim 100\text{km}$ ), the land  
296 surface simulation driven by bias corrected CMIP6 results (CMIP6\_His/CSSPv2) also  
297 captures the terrestrial hydrological variations reasonably well. The Kling-Gupta  
298 efficiency of the ensemble mean streamflow simulation reaches up to 0.71~0.81, and  
299 the ensemble mean monthly Terrestrial Water Storage Anomaly (TWSA) and annual

300 evapotranspiration generally agree with observations and other reference data  
301 (Figures 23c-3d).

302 Figure 34 shows relative changes of terrestrial hydrological variables over the  
303 Sanjiangyuan region at different warming levels. The ensemble mean of the increase  
304 in annual precipitation is 5% at 1.5°C warming level, and additional 0.5°C and 1.5°C  
305 warming will further increase the wetting trends to 7% and 13% respectively. Annual  
306 evapotranspiration experiences significant increases at all warming levels, and the  
307 ensemble mean increases are 4%, 7% and 13% at 1.5, 2.0 and 3.0°C warming levels  
308 respectively. The ratio of transpiration to evapotranspiration also increases  
309 significantly, indicating that vegetation transpiration increases much larger than the  
310 soil evaporation and canopy evaporation. Although annual total runoff has larger  
311 relative changes than evapotranspiration (6%, 9% and 14% at 1.5, 2.0 and 3.0°C  
312 warming levels respectively), the uncertainty is large as only 75% of the models show  
313 positive signals, which may be caused by large uncertainty in the changes during  
314 summer and autumn seasons. The terrestrial water storage (TWS) which includes  
315 foliage water, surface water, soil moisture and groundwater, shows slightly decreasing  
316 trend at ~~both annual and seasonal scales, however, changes little at the three warming~~  
317 ~~levels,~~ suggesting that the increasing precipitation in the future becomes extra  
318 evapotranspiration and runoff instead of recharging the local water storage. The  
319 accelerated terrestrial hydrological cycle also exists at seasonal scale, as the seasonal  
320 changes are consistent with the annual ones.

321 **3.2 Changes in streamflow extremes at different warming levels**

322        Although the intensified terrestrial hydrology induces more streamflow over the  
323        headwater region of Yellow river during winter and spring months, streamflow does  
324        not increase and even decreases during the flood season (July-September; Figure 45a).

325        Figure 5b shows the changes of streamflow dry extremes over the Yellow river source  
326        region at different warming levels, with the error bars showing estimated uncertainties.

327        ~~Moreover, the frequency of streamflow dry extremes over the Yellow river is found~~  
328        to increase by 55% at 1.5°C warming level (Figure 45b), but the uncertainty is larger  
329        than the ensemble mean. However, suggesting that abnormally low streamflow will  
330        ~~occur more frequently during the flood seasons in the future.~~ The dry extreme  
331        frequency will further increase to 77% and 125% at the 2.0 and 3.0°C warming levels  
332        and the results ~~become are more~~ significant (Figure 45b). No statistically significant  
333        changes are found for the wet extremes at all warming levels over the Yellow River  
334        headwater region, as the uncertainty ranges are larger than the ensemble means.

335        Over the Yangtze river headwater region, streamflow increases in all months at  
336        different warming levels (Figure 45c). The frequency of wet extremes increases  
337        significantly by 138%, 202% and 232% at 1.5, 2.0 and 3.0°C warming levels (Figure  
338        45d), suggesting a higher risk of flooding. ~~Moreover~~Although, the frequency of dry  
339        extremes also tends to decrease significantly by 35%, 44%, 34% at the three warming  
340        levels, ~~but~~ the changes are much smaller than those of the wet extremes. Moreover,  
341        contributions from climate change and ecological change are both smaller than the  
342        uncertainty ranges (not shown), suggesting that their impacts on the changes of dry  
343        extremes over the Yangtze river headwater region are not distinguishable. Thus, we

344 mainly focus on the dry extremes over the Yellow river and the wet extremes over the  
345 Yangtze river in the following analysis.

346 Different changes of streamflow extremes over the Yellow and Yangtze rivers  
347 can be interpreted from different accelerating rates of precipitation and  
348 evapotranspiration. Figure 56 shows probability density functions (PDFs) of  
349 precipitation, evapotranspiration and their difference (P-ET, i.e. residual water for  
350 runoff generation) during the flood season. Over the Yellow river, PDFs of  
351 precipitation and evapotranspiration both shift to the right against the reference period,  
352 except for the precipitation at 1.5°C warming level. However, the increasing trend of  
353 evapotranspiration is stronger than that of precipitation, leading to a left shift of PDF  
354 for P-ET. Moreover, increased variations of precipitation and evapotranspiration, as  
355 indicated by the increased spread of their PDFs, also lead to a larger spread of PDFs  
356 of P-ET. The above two factors together induce a heavier left tail in the PDF of P-ET  
357 for the warming future than the reference period (Figure 56e). The probability of  
358 P-ET<80mm increases from 0.1 during historical period to 0.11, 0.13 and 0.16 at 1.5,  
359 2.0 and 3.0°C warming levels individually. This indicates a higher probability of less  
360 water left for runoff generation at different warming levels, given little changes in  
361 TWS (section 3.1). Moreover, Figure 36e also shows little change to the right tails in  
362 the PDF of P-ET as probability for P-ET>130mm stays around 0.1 (P-ET>130mm) at  
363 different warming levels, suggesting little change to the probability of high residual  
364 water. This is consistent with the insignificant wet extreme change over the Yellow  
365 river. Over the Yangtze river, however, intensified evapotranspirationprecipitation is

366 much largersmaller than the increased evapotranspirationprecipitation, leading to a  
367 systematic rightward shift of the PDF of P-ET (Figures 56b, 56d and 56f). Thus both  
368 the dry and wet extremes show significant changes over the Yangtze river.

369 **3.3 Influences of land cover change and CO<sub>2</sub> physiological forcing**

370 Figures 67a-67b show the changes of streamflow extremes (compared with the  
371 reference period) induced by climate and ecological factors. Although the contribution  
372 from climate change (red bars in Figures 7a-7b) is greater than the ecological factors  
373 (blue and cyan bars in in Figures 7a-7b), influences of CO<sub>2</sub> physiological forcing and  
374 land cover change are nontrivial. The CO<sub>2</sub> physiological forcing tends to alleviate dry  
375 extremes (or increase wet extremes), while land cover change plays a contrary role.  
376 Over the Yellow river, the combined impact of the two ecological factors (sum of blue  
377 and cyan bars) reduces the increasing trend of dry extremes caused by climate change  
378 (red bars) by 18~22% at 1.5 and 2.0 °C warming levels, while intensifies the dry  
379 extremes by 9% at 3.0°C warming level. This can be interpreted from their  
380 contributions to the evapotranspiration, as the increased LAI enhancement on ET is  
381 weaker than the suppression effect of CO<sub>2</sub> physiological impact at 1.5 and 2.0°C  
382 warming levels, while stronger at 3.0°C warming level (not shown). Over the Yangtze  
383 river, similarly, combined effect of land cover and CO<sub>2</sub> physiological forcing  
384 increases the wet extremes by 9% at 1.5°C warming level while decreases the wet  
385 extremes by 12% at 3.0°C warming level. Thus, although contribution from climate  
386 change is greater than the ecological factors, plays the dominate role in inducing the  
387 extreme changes at different warming levels, influences of CO<sub>2</sub> physiological forcing

388 and land cover change are nontrivial.

389 In addition, Figures 67c and 67d show that the combined impact of CO<sub>2</sub>  
390 physiological forcing and land cover change also influences the differences between  
391 different warming levels. Over the Yellow river, climate change increases dry  
392 extremes by 26% from 1.5 to 2.0°C warming level, and by 40% from 1.5 and 3.0°C  
393 warming level (red bars in Figure 67c). After considering the two ecological factors  
394 (pink bars in Figure 67c), above two values change to 22% and 70% respectively, and  
395 the difference between 1.5 and 3.0°C warming levels becomes significant. For the wet  
396 extreme over the Yangtze river (Figure 67d), the climate change induced difference  
397 between 1.5 and 2.0°C warming levels is decreased by 16% after accounting for the  
398 two ecological factors. And this decrease reaches up to 49% for the difference  
399 between 1.5 and 3.0°C warming levels. We also compared the scenarios when CO<sub>2</sub>  
400 physiological forcing and land cover change are combined with climate change  
401 individually (blue and cyan bars in Figures 67c-d), and the results show the land cover  
402 change dominates their combined influences on the difference between different  
403 warming levels.

404 **4 Conclusions and Discussion**

405 This study investigates changes of streamflow extremes over the Sanjiangyuan  
406 region at different global warming levels through high-resolution land surface  
407 modeling driven by CMIP6 climate simulations. The terrestrial hydrological cycle  
408 under global warming of 1.5°C is found to accelerate by 4~6% compared with the  
409 reference period of 1985-2014, according to the relative changes of precipitation,

410 evapotranspiration and total runoff. The terrestrial water storage, however, shows a  
411 slight but significant decreasing trend as increased evapotranspiration and runoff are  
412 larger than the increased precipitation. This decreasing trend of terrestrial water  
413 storage in the warming future is also found in six major basins in China (Jia et al.,  
414 2020). Although streamflow changes during the flood season has a large uncertainty,  
415 the frequency of wet extremes over the Yangtze river will increase significantly by  
416 138% and that of dry extremes over the Yellow river will increase by 55% compared  
417 with that during 1985~2014. With an additional 0.5°C warming, the frequency of dry  
418 and wet extremes will increase further by 22~64%. If the global warming is not  
419 adequately managed (e.g., to reach 3.0°C), wet extremes over the Yangtze river and  
420 dry extremes over the Yellow river will increase by 232% and 125%. ~~These~~  
421 nonlineare changes from 1.5 to 2.0 and 3.0°C are nonlinear compared with that from  
422 reference period to 1.5°C, which are also found for some fixed-threshold climate  
423 indices over the Europe (Dosio and Fischer, 2018). It is necessary to cap the global  
424 warming at 2°C or even lower level, to reduce the risk of wet and dry extremes over  
425 the Yangtze and Yellow rivers.

426 This study also shows the nontrivial contributions from land cover change and  
427 CO<sub>2</sub> physiological forcing to the extreme streamflow changes especially at 2.0 and  
428 3.0°C warming levels. The CO<sub>2</sub> physiological forcing is found to increase streamflow  
429 and reduce the dry extreme frequency by 14~24%, which is consistent with previous  
430 research that CO<sub>2</sub> physiological forcing would increase available water and reduce  
431 water stress at the end of this century (Wiltshire et al., 2013). However, our results

432 further show that the drying effect of increasing LAI on streamflow will exceed the  
433 wetting effect of CO<sub>2</sub> physiological forcing at 3.0°C warming level (during  
434 2048~2075) over the Sanjiangyuan region, making a reversion in the combined  
435 impacts of CO<sub>2</sub> physiological forcing and land cover. Thus it is vital to consider the  
436 impact of land cover change in the projection of future water stress especially at high  
437 warming scenarios.

438 Moreover, about 43~52% of the extreme streamflow changes between 1.5 and  
439 3.0°C warming levels are attributed to the increased LAI. Considering the LAI  
440 projections from different CMIP6 models are induced by the climate change, it can be  
441 inferred that the indirect influence of climate change (e.g., through land cover change)  
442 has the same and even larger importance on the changes of streamflow extremes  
443 between 1.5 and 3.0°C or even higher warming levels, compared with the direct  
444 influence (e.g., through precipitation and evapotranspiration). Thus, it is vital to  
445 investigate hydrological and its extremes changes among different warming levels  
446 from an eco-hydrological perspective instead of focusing on climate change alone.

447 Although we used 11 CMIP6 models combined with two SSP scenarios to reduce  
448 the uncertainty of future projections caused by GCMs, using a single land surface  
449 model may result in uncertainties (Marx et al., 2018). However, considering the good  
450 performance of the CSSPv2 land surface model over the Sanjiangyuan region and the  
451 dominant role of GCMs' uncertainty (Zhao et al., 2019; Samaniego et al., 2017),  
452 uncertainty from the CSSPv2 model should have limited influence on the robust of  
453 the result.

454

455 **Acknowledgments** We thank the World Climate Research Programme's Working

456 Group on Couple modelling for providing CMIP6 data (<https://esgf-node.llnl.gov>).

457 This work was supported by National Key R&D Program of China

458 (2018YFA0606002) and National Natural Science Foundation of China (41875105,

459 91547103), and the Startup Foundation for Introducing Talent of NUIST.

460

461 **Competing interests**

462 The authors declare that they have no conflict of interest.

463

464 **References**

465 Bibi, S., Wang, L., Li, X., Zhou, J., Chen, D., and Yao, T.: Climatic and associated  
466 cryospheric, biospheric, and hydrological changes on the Tibetan Plateau: a

467 review, Int. J. Climatol., 38, e1-e17, <https://doi.org/10.1002/joc.5411>, 2018.

468 Chen, J., Gao, C., Zeng, X., Xiong, M., Wang, Y., Jing, C. Krysanova, V., Huang, J.,  
469 Zhao, N., and Su, B.: Assessing changes of river discharge under global warming  
470 of  $1.5^{\circ}$  C and  $2^{\circ}$  C in the upper reaches of the Yangtze River Basin: Approach  
471 by using multiple-GCMs and hydrological models, Quatern. Int., 453, 1 – 11,  
472 <http://dx.doi.org/10.1016/j.quaint.2017.01.017>, 2017.

473 Cuo, L., Zhang, Y., Zhu, F., and Liang, L.: Characteristics and changes of streamflow  
474 on the Tibetan Plateau: A review, J. Hydrol.-Reg. Stud., 2, 49 – 68,  
475 <https://doi.org/10.1016/j.ejrh.2014.08.004>, 2014.

476 Dai, Y. J., Zeng, X. B., Dickinson, R. E., Baker, I., Bonan, G. B., Bosilovich, M. G.,  
477 Denning, A. S., Dirmeyer, P. A., Houser, P. R., Niu, G. Y., Oleson, K. W.,  
478 Schlosser, C. A., and Yang, Z. L.: The Common Land Model. B. Am. Meteorol.  
479 Soc., 84, 1013 – 1024, <https://doi.org/10.1175/BAMS-84-8-1013>, 2003.

480 Döll, P., Trautmann, T., Gerten, D., Schmied, H. M., Ostberg, S., Saaed, F., and  
481 Schleussner, C.: Risks for the global freshwater system at  $1.5^{\circ}$  C and  $2^{\circ}$  C  
482 global warming. Environ. Res. Lett., 13, 044038,  
483 <https://doi.org/10.1088/1748-9326/aab792>, 2018.

484 Dosio, A., and Fischer, E. M.: Will half a degree make a difference? Robust  
485 projections of indices of mean and extreme climate in Europe under  $1.5^{\circ}$  C,  $2^{\circ}$

486 C, and 3 ° C global warming, Geophys. Res. Lett., 45.

487 <https://doi.org/10.1002/2017GL076222>, 2018.

488 Eyring, V., Bony, S., Meehl, G. A., Senior, C. A., Stevens, B., Stouffer, R. J., and

489 Taylor, K. E.: Overview of the Coupled Model Intercomparison Project Phase 6

490 (CMIP6) experimental design and organization, Geosci. Model Dev., 9, 1937 –

491 1958. <https://doi.org/10.5194/gmd-9-1937-2016>, 2016.

492 Fowler, M. D., Kooperman G. J., Randerson, J. T. and Pritchard M. S.: The effect of

493 plant physiological responses to rising CO<sub>2</sub> on global streamflow, Nat. Clim.

494 Change, 9, 873-879, https://doi.org/10.1038/s41558-019-0602-x, 2019.

495 He, J., Yang, K., Tang, W., Lu, H., Qin, J., Chen, Y., and Li, X.: The first

496 high-resolution meteorological forcing dataset for land process studies over

497 China, Sci. Data, 7, 25. <https://doi.org/10.1038/s41597-020-0369-y>, 2020.

498

499 Hempel, S., Frieler, K., Warszawski, L., and Piontek, F.: A trend-preserving bias

500 correction-the ISI-MIP approach, Earth Syst. Dyn., 4, 219-236.

501 <https://doi.org/10.5194/esd-4-219-2013>, 2013.

502 Ji, P., and Yuan, X.: High-resolution land surface modeling of hydrological changes

503 over the Sanjiangyuan region in the eastern Tibetan Plateau: 2. Impact of climate

504 and land cover change, J. Adv. Model. Earth. Sy., 10, 2829 – 2843.

505 <https://doi.org/10.1029/2018MS001413>, 2018.

506 Jia, B., Cai, X., Zhao, F., Liu, J., Chen, S., Luo, X., Xie, Z., and Xu, J.: Potential

507 future changes of terrestrial water storage based on climate projections by

508 [ensemble model simulations, \*Adv. Water Resour.\*, 142, 103635.](https://doi.org/10.1016/j.advwatres.2020.103635)  
509 [https://doi.org/10.1016/j.advwatres.2020.103635, 2020.](https://doi.org/10.1016/j.advwatres.2020.103635)

510 Jung, M., Reichstein, M., and Bondeau, A.: Towards global empirical upscaling of  
511 FLUXNET eddy covariance observations: Validation of a model tree ensemble  
512 approach using a biosphere model, *Biogeosciences*, 6, 2001–2013.  
513 [https://doi.org/10.5194/bg-6-2001-2009, 2009.](https://doi.org/10.5194/bg-6-2001-2009)

514 Kuang, X., and Jiao, J.: Review on climate change on the Tibetan Plateau during the  
515 last half century, *J. Geophys. Res. Atmos.*, 121, 3979 – 4007.  
516 [https://doi.org/10.1002/2015JD024728, 2016.](https://doi.org/10.1002/2015JD024728)

517 [Li, J., Liu, D., Li, Y., Wang, S., Yang, Y., Wang, X., Guo, H., Peng, S., Ding, J., Shen, M., and Wang, L.: Grassland restoration reduces water yield in the headstream region of Yangtze River, \*Sci. Rep.\*, 7, 2162,](https://doi.org/10.1038/s41598-017-02413-9)  
518 <https://doi.org/10.1038/s41598-017-02413-9, 2017.>

520

521 Li, W., Jiang, Z., Zhang, X., Li, L. and Sun, Y.: Additional risk in extreme  
522 precipitation in China from 1.5 ° C to 2.0 ° C global warming levels, *Sci.  
523 Bull.*, 63, 228. [https://doi.org/10.1016/j.scib.2017.12.021, 2018.](https://doi.org/10.1016/j.scib.2017.12.021)

524 Liang, L., Li, L., Liu, C., and Cuo, L.: Climate change in the Tibetan Plateau Three  
525 Rivers Source Region: 1960 – 2009, *Int. J. Climatol.*, 33, 2900-2916.  
526 [https://doi.org/10.1002/joc.3642, 2013.](https://doi.org/10.1002/joc.3642)

527 [Liang, X., Lettenmaier, D. P., Wood, E. F., and Burges, S. J.: A simple hydrologically  
528 based model of land surface water and energy fluxes for general circulation](https://doi.org/10.1038/s41598-017-02413-9)

529 [models, J. Geophys. Res., 99, 14,415-14,428. https://doi.org/10.1029/94JD00483,](https://doi.org/10.1029/94JD00483)  
530 [1994.](https://doi.org/10.1029/94JD00483)

531 Marcott, S. A., Shakun, J. D., Clark, P. U., and Mix, A. C.: A Reconstruction of  
532 Regional and Global Temperature for the Past 11,300 Years, *Science*, 339, 1198  
533 – 1201. <https://doi.org/10.1126/science.1228026>, 2013.

534 Martens, B., Miralles, D. G., Lievens, H., van der Schalie, R., de Jeu, R. A. M.,  
535 Fernández-Prieto, D., Beck, H. E., Dorigo, W. A., and Verhoest, N. E. C.:  
536 GLEAM v3: satellite-based land evaporation and root-zone soil moisture, *Geosci.*  
537 *Model Dev.*, 10, 1903–1925. <https://doi.org/10.5194/gmd-10-1903-2017>, 2017.

538 Marx, A., Kumar, R., and Thober, S.: Climate change alters low flows in Europe  
539 under global warming of 1.5, 2, and 3 ° C, *Hydrol. Earth. Syst. Sc.*, 22, 1017 –  
540 1032. <https://doi.org/10.5194/hess-22-1017-2018>, 2018.

541 [Meinshausen, M., Nicholls, Z. R. J., Lewis, J., Gidden, M. J., Vogel, E., Freund, M.,](https://doi.org/10.5194/gmd-13-3571-2020)  
542 [Beyerle, U., Gessner, C., Nauels, A., Bauer, N., Canadell, J. G., Daniel, J. S.,](https://doi.org/10.5194/gmd-13-3571-2020)  
543 [John, A., Krummel, P. B., Luderer, G., Meinshausen, N., Montzka, S. A., Rayner,](https://doi.org/10.5194/gmd-13-3571-2020)  
544 [P. J., Reimann, S., Smith, S. J., van den Berg, M., Velders, G. J. M., Vollmer, M.](https://doi.org/10.5194/gmd-13-3571-2020)  
545 [K., and Wang, R. H. J.: The shared socio-economic pathway \(SSP\) greenhouse](https://doi.org/10.5194/gmd-13-3571-2020)  
546 [gas concentrations and their extensions to 2500, \*Geosci. Model Dev.\*, 13, 3571 –](https://doi.org/10.5194/gmd-13-3571-2020)  
547 [3605, https://doi.org/10.5194/gmd-13-3571-2020, 2020.](https://doi.org/10.5194/gmd-13-3571-2020)

548 Meinshausen, M., Vogel, E., and Nauels, A., [Lorbacher, K., Meinshausen, N.,](https://doi.org/10.5194/gmd-13-3571-2020)  
549 [Etheridge, D. M., Fraser, P. J., Montzka, S. A., Rayner, P. J., Trudinger, C. M.,](https://doi.org/10.5194/gmd-13-3571-2020)  
550 [Krummel, P. B., Beyerle, U., Canadell, J. G., Daniel, J. S., Enting, I. G., Law, R.](https://doi.org/10.5194/gmd-13-3571-2020)

M., Lunder, C. R., O'Doherty, S., Prinn, R. G., Reimann, S., Rubino, M., Velders, G. J. M., Vollmer, M. K., Wang, R. H. J., and Weiss, R.: Historical greenhouse gas concentrations for climate modelling (CMIP6), *Geosci. Model Dev.*, 10, 2057-2116. <https://doi.org/10.5194/gmd-10-2057-2017>, 2017.

Mohammed, K., Islam, A. S., Islam, G. M. T., Alfieri, L., Bala, S. K., and Khan, M. J. U.: Extreme flows and water availability of the Brahmaputra River under 1.5 and 2 ° C global warming scenarios, *Climatic Change*, 145, 159-175. <https://doi.org/10.1007/s10584-017-2073-2>, 2017.

Morice, C. P., Kennedy J. J., Rayner N. A., and Jones P. D.: Quantifying uncertainties in global and regional temperature change using an ensemble of observational estimates: The HadCRUT4 dataset, *J. Geophys. Res.*, 117, D08101. <https://doi.org/10.1029/2011JD017187>, 2012.

Oleson, K. W., Lawrence, D. M., Bonan, G. B., Drewniak, B., Huang, M., Koven, C.  
D., Levis, S., Li, F., Riley, W. J., Subin, Z. M., Swenson, S. C., Thornton, P. E.,  
Bozbiyik, A., Fisher, R., Heald, C. L., Kluzeck, E., Lamarque, J. F., Lawrence, P.  
J., Leung, L. R., Lipscomb, W., Muszala, S., Ricciuto, D. M., Sacks, W., Sun, Y.,  
Tang, J., Yang, Z. L.: Technical description of version 4.5 of the Community  
Land Model (CLM) (Rep. NCAR/TN-503 + STR, 420), 2013.

O'Neill, B. C., Tebaldi, C., Vuuren, D. P. V., Eyring, V., Friedlingstein, P., Hurtt, G., Knutti, R., Kriegler, E., Lamarque, J. F., Lowe, J., Meehl, G. A., Moss, R., Riahi, K., and Sanderson, B. M.: The scenario model intercomparison project

572 (ScenarioMIP) for CMIP6, Geosci. Model Dev., 9, 3461-3482.

573 <https://doi.org/10.5194/gmd-9-3461-2016>, 2016.

574 Samaniego, L., Kumar, R., Breuer, L., Chamorro, A., Flörke, M., Pechlivanidis, I. G.,

575 Schäfer, D., Shah, H., Vetter, T., Wortmann, M., and Zeng, X.: Propagation of

576 forcing and model uncertainties on to hydrological drought characteristics in a

577 multi-model century-long experiment in large river basins, Climatic Change, 141,

578 435-449. https://doi.org/10.1007/s10584-016-1778-y, 2017.

579 Thober, T., Kumar, R., and Wadens, N.: Multi-model ensemble projections of

580 European river floods and high flows at 1.5, 2, and 3 degrees global warming,

581 Environ. Res. Lett., 13, 014003. <https://doi.org/10.1088/1748-9326/aa9e35>,

582 2018.

583 Vicente-Serrano, S. M., Lopez-Moreno, J. I., Begueria, S., Lorenzo-Lacruz, J.,

584 Azorin-Molina, C., and Moran-Tejeda, E.: Accurate computation of a streamflow

585 drought index, J. Hydrol. Eng., 17, 318 – 332.

586 [https://doi.org/10.1061/\(ASCE\)He.1943-5584.0000433](https://doi.org/10.1061/(ASCE)He.1943-5584.0000433), 2012.

587 Watkins, M. M., Wiese, D. N., Yuan, D. N., Boening, C., and Landerer, F. W.:

588 Improved methods for observing Earth's time variable mass distribution with

589 GRACE using spherical cap mascons, J. Geophys. Res. Solid Earth, 120,

590 2648-2671. <https://doi.org/10.1002/2014JB011547>, 2015.

591 Wiltshire, A., Gornall, J., Booth, B., Dennis, E., Falloon, P., Kay, G., McNeall, D.,

592 McSweeney, C. and Betts, R.: The importance of population, climate change and

593 CO<sub>2</sub> plant physiological forcing in determining future global water stress, Global

594 Environ. Change, 23(5), 1083-1097.

595 <http://dx.doi.org/10.1016/j.gloenvcha.2013.06.005>, 2013.

596 WMO.: WMO Statement on the State of the Global Climate in 2019,

597 [https://library.wmo.int/doc\\_num.php?explnum\\_id=10211](https://library.wmo.int/doc_num.php?explnum_id=10211), 2020.

598 Yang, K., Wu, H., Qin, J., Lin, C., Tang, W., and Chen, Y.: Recent climate changes

599 over the Tibetan plateau and their impacts on energy and water cycle: A review,

600 Global Planet. Change, 112, 79 - 91.

601 <https://doi.org/10.1016/j.gloplacha.2013.12.001>, 2013.

602 Yang, Y., Rodericj, M. L., Zhang, S., McVicar, T. R., and Donohue, R. J.: Hydrologic

603 implications of vegetation response to elevated CO<sub>2</sub> in climate projections, Nat.

604 Clim. Change, 9, 44-48. <https://doi.org/10.1038/s41558-018-0361-0>, 2019.

605 Yuan, X., Ji, P., Wang, L., Liang, X., Yang, K., Ye, A., Su, Z., and Wen, J.: High

606 resolution land surface modeling of hydrological changes over the Sanjiangyuan

607 region in the eastern Tibetan Plateau: 1. Model development and evaluation, J.

608 Adv. Model. Earth. Sy., 10, 2806 - 2828. <https://doi.org/10.1029/2018MS001413>,

609 2018a.

610 Yuan, X., Jiao, Y., Yang, D., and Lei, H.: Reconciling the attribution of changes in

611 streamflow extremes from a hydroclimate perspective, Water Resour. Res., 54,

612 3886 - 3895. <https://doi.org/10.1029/2018WR022714>, 2018b.

613 Yuan, X., Zhang, M., Wang, L., and Zhou, T.: Understanding and seasonal forecasting

614 of hydrological drought in the Anthropocene, Hydrol. Earth. Syst. Sc., 21, 5477

615 - 5492. <https://doi.org/10.5194/hess-21-5477-2017>, 2017.

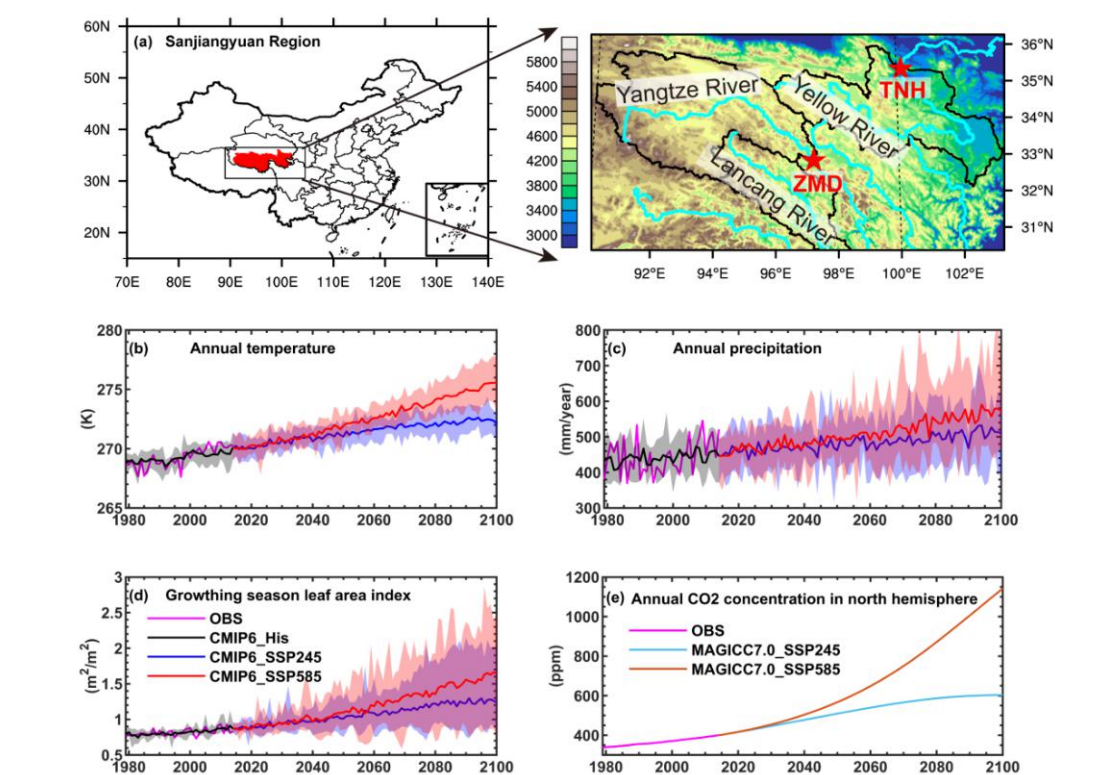
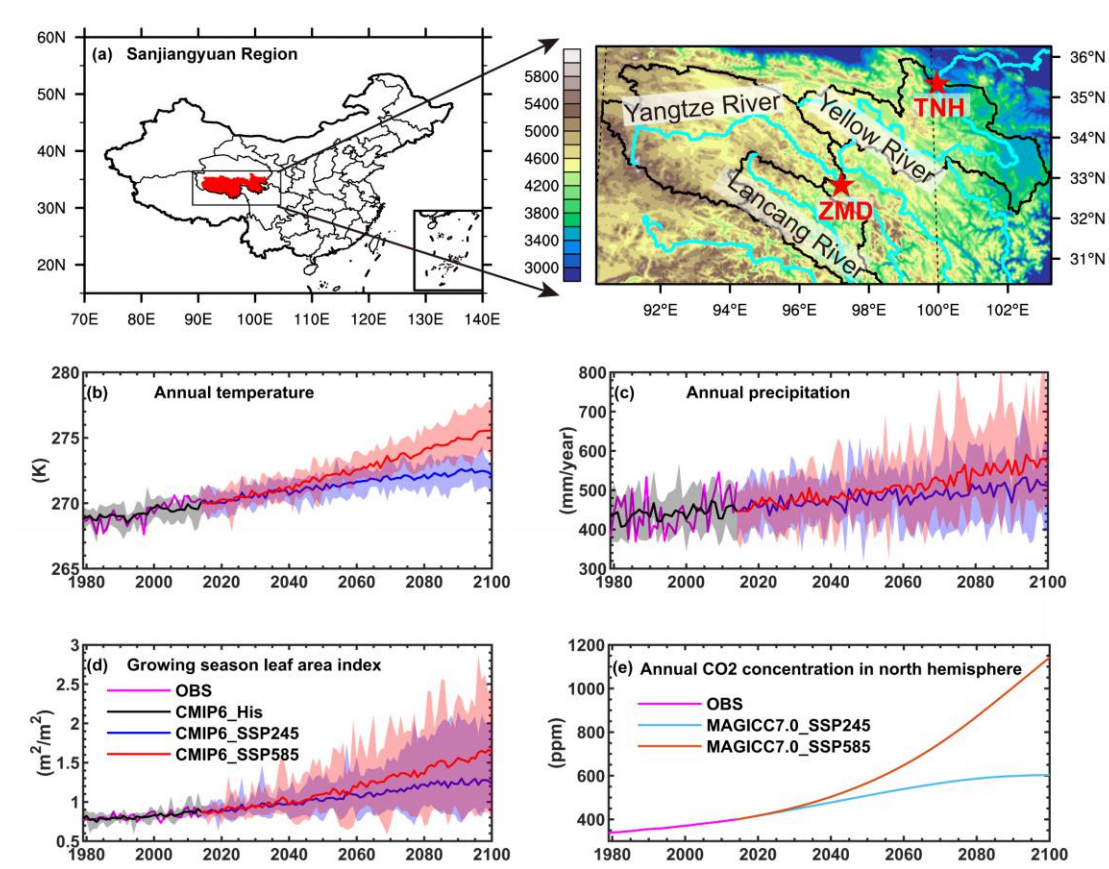
616 Zhang Y., You Q., Chen C., and Ge J.: Impacts of climate change on streamflows  
617 under RCP scenarios: A case study in Xin River Basin, China, *Atmos. Res.*,  
618 178-179, 521-534. <http://dx.doi.org/10.1016/j.atmosres.2016.04.018>, 2016.

619 Zhao Q., Ding Y., Wang J., Gao H., Zhang S., Zhao C. Xu J. Han H., and Shangguan  
620 D.: Projecting climate change impacts on hydrological processes on the Tibetan  
621 Plateau with model calibration against the glacier inventory data and observed  
622 streamflow, *J. Hydrol.*, 573, 60-81. <https://doi.org/10.1016/j.jhydrol.2019.03.043>,  
623 2019.

624 Zhu Q., Jiang H., Peng C., Liu J., Fang X., Wei X., Liu S., and Zhou G.: Effects of  
625 future climate change, CO<sub>2</sub> enrichment, and vegetation structure variation on  
626 hydrological processes in China, *Global Planet. Change*, 80-81, 123-135.  
627 <https://doi.org/10.1016/j.gloplacha.2011.10.010>, 2012.

628 Zhu, Z. C., Piao, S. L., Myneni, R. B., Huang, M. T., Zeng, Z. Z., Canadell, J. G.,  
629 Ciais, P., Sitch, S., Friedlingstein, P., Arneth, A., Cao, C. X., Cheng, L., Kato, E.,  
630 Koven, C., Li, Y., Lian, X., Liu, Y. W., Liu, R. G., Mao, J. F., Pan, Y. Z., Peng, S.,  
631 S., Penuelas, J., Poulter, B., Pugh, T. A. M., Stocker, B. D., Viovy, N., Wang, X.  
632 H., Wang, Y. P., Xiao, Z. Q., Yang, H., Zaehle, S., and Zeng, N.: Greening of the  
633 Earth and its drivers, *Nature Climate Change*, 6(8), 791-+,  
634 <https://doi.org/10.1038/Nclimate3004>, 2016.

635



638 **Figure 1.** (a) The locations of the Sanjiangyuan region and streamflow gauges. (b)-(e)

639 are the time series of annual temperature, precipitation, growing season leaf area

640 index and CO<sub>2</sub> concentration averaged over the Sanjiangyuan region during  
641 1979-2100. Red pentagrams in (a) are two streamflow stations named Tangnaihai  
642 (TNH) and Zhimenda (ZMD). Black, blue and red lines in (b-d) are ensemble means  
643 of CMIP6 model simulations from the historical, SSP245 and SSP585 experiments.  
644 Shadings are ranges of individual ensemble members. Cyan and brown lines in (e) are  
645 future CO<sub>2</sub> concentration under SSP245 and SSP585 scenarios simulated by  
646 MAGICC7.0 model.

647

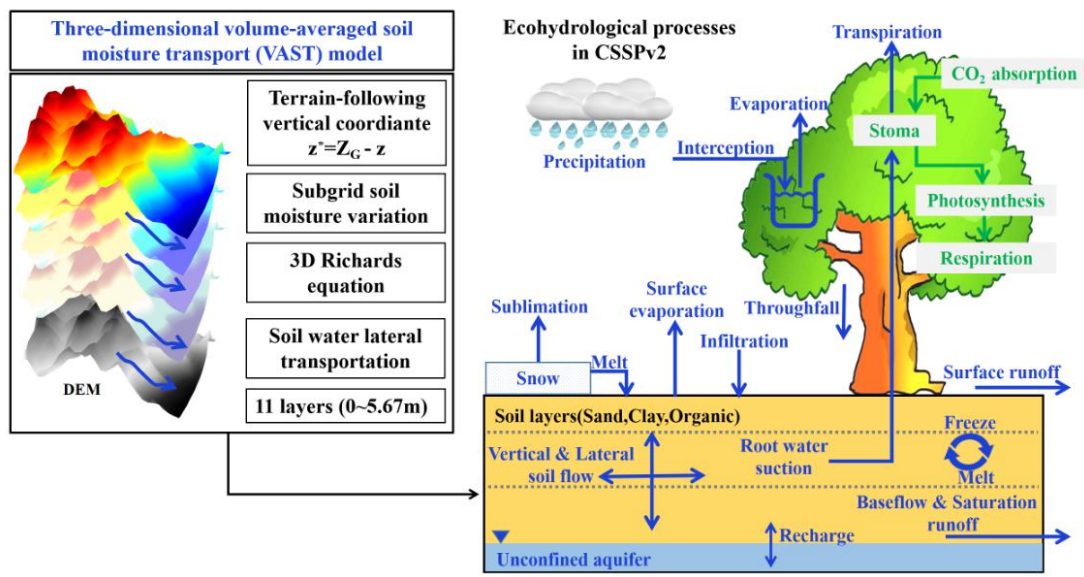


**Figure 2. Main ecohydrological processes in the Conjunctive Surface-Subsurface Process version 2 (CSSPv2) land surface model.**

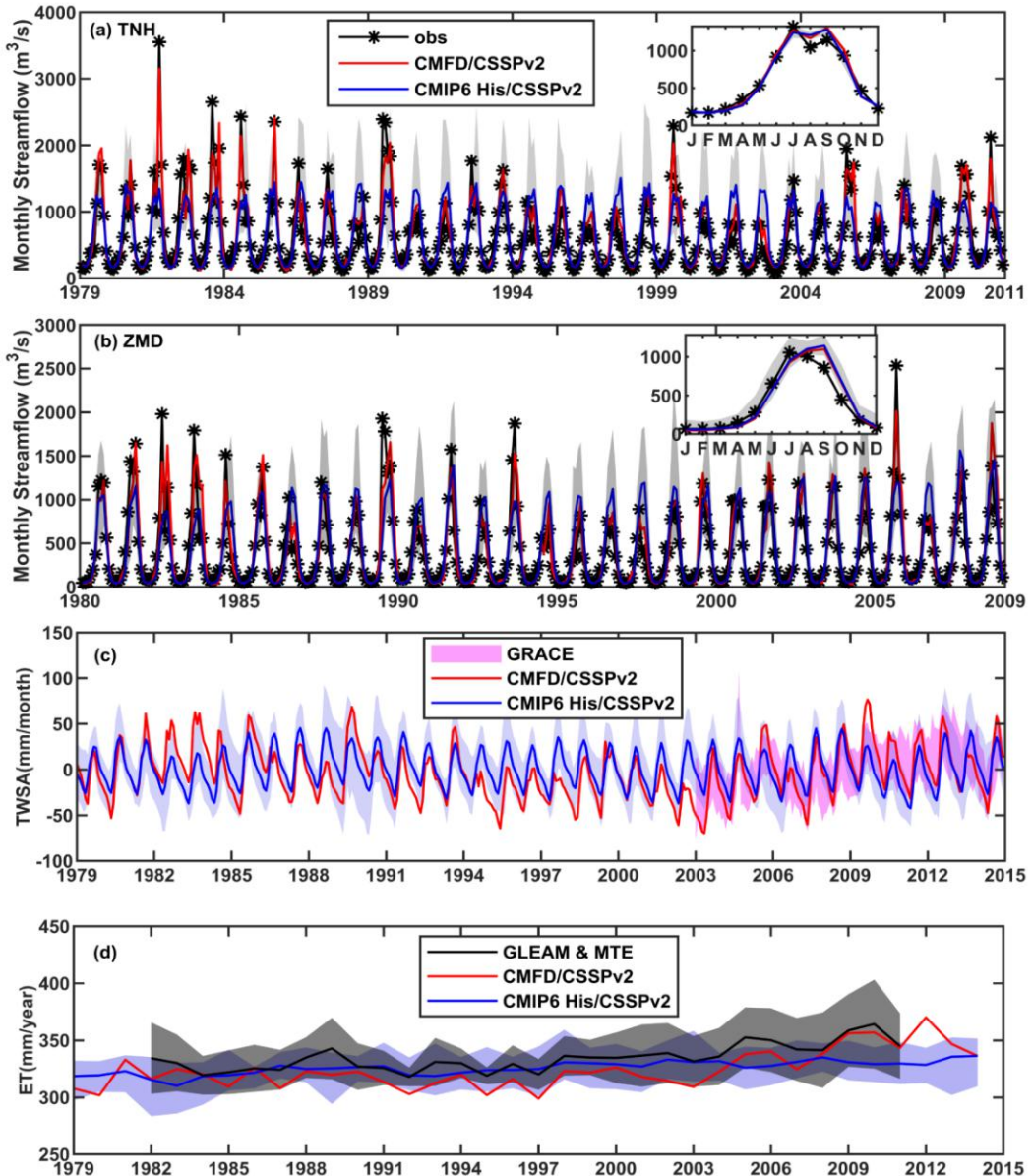


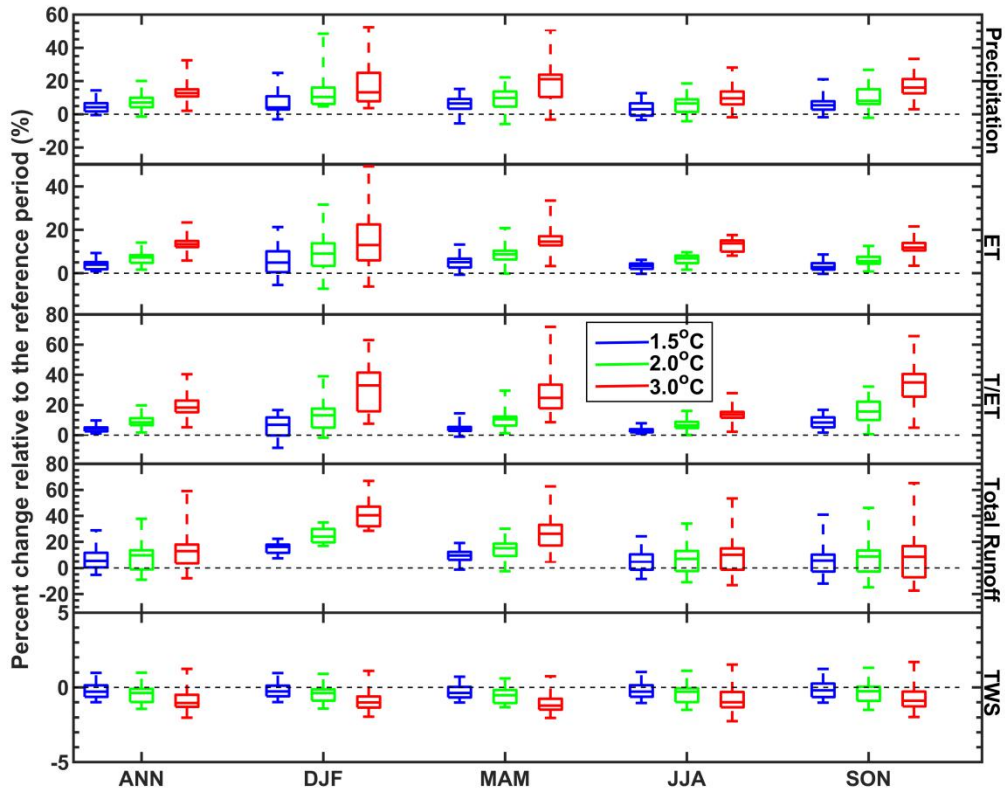
**Figure 23.** Evaluation of model simulations. (a-b) Observed and simulated monthly

streamflow at the Tangnaihai (TNH) and Zhimenda (ZMD) hydrological stations, with the climatology shown in the upper-right corner. (c-d) Evaluation of the simulated monthly terrestrial water storage anomaly (TWSA) and annual evapotranspiration (ET) averaged over the Sanjiangyuan region. Red lines are CSSPv2 simulation forced by observed meteorological forcing. Blue lines represent ensemble means of 11 CMIP6\_His/CSSPv2 simulations, while gray shadings in (a-b) and blue shadings in (c-d) are ranges of individual ensemble members. Pink shading in (c) is GRACE

661 satellite observations. Black line and black shading in (d) are ensemble mean and  
662 ranges of GLEAM\_ET and MTE\_ET datasets.

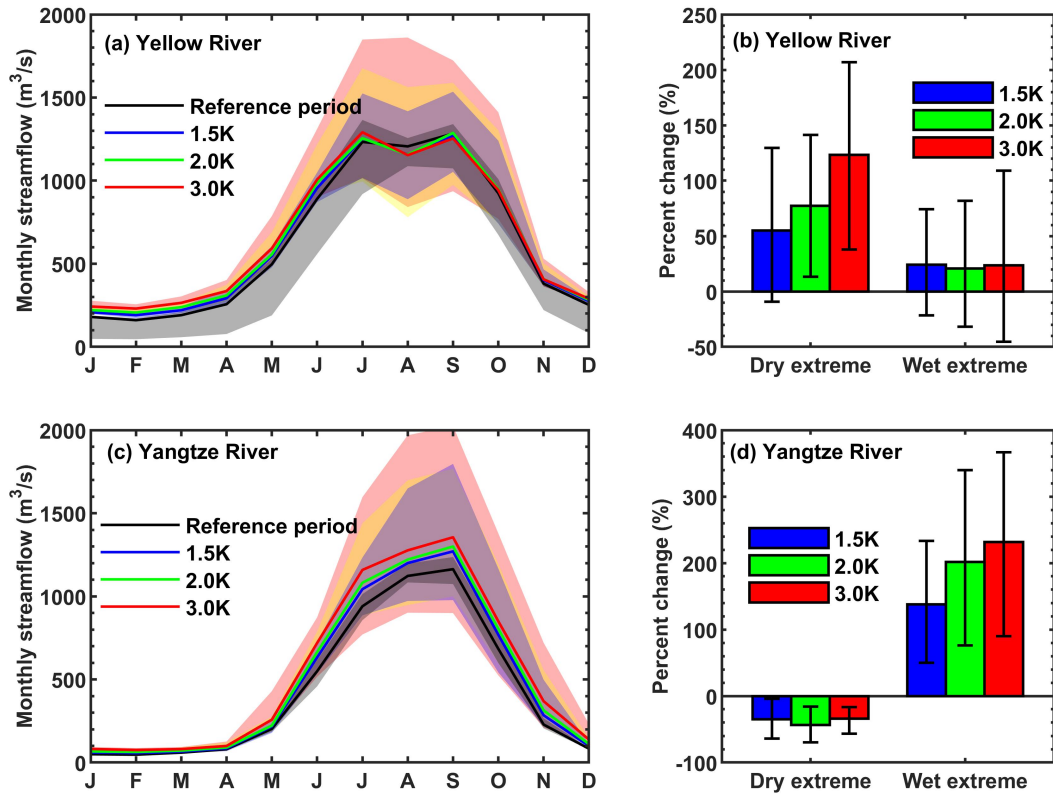
663

664

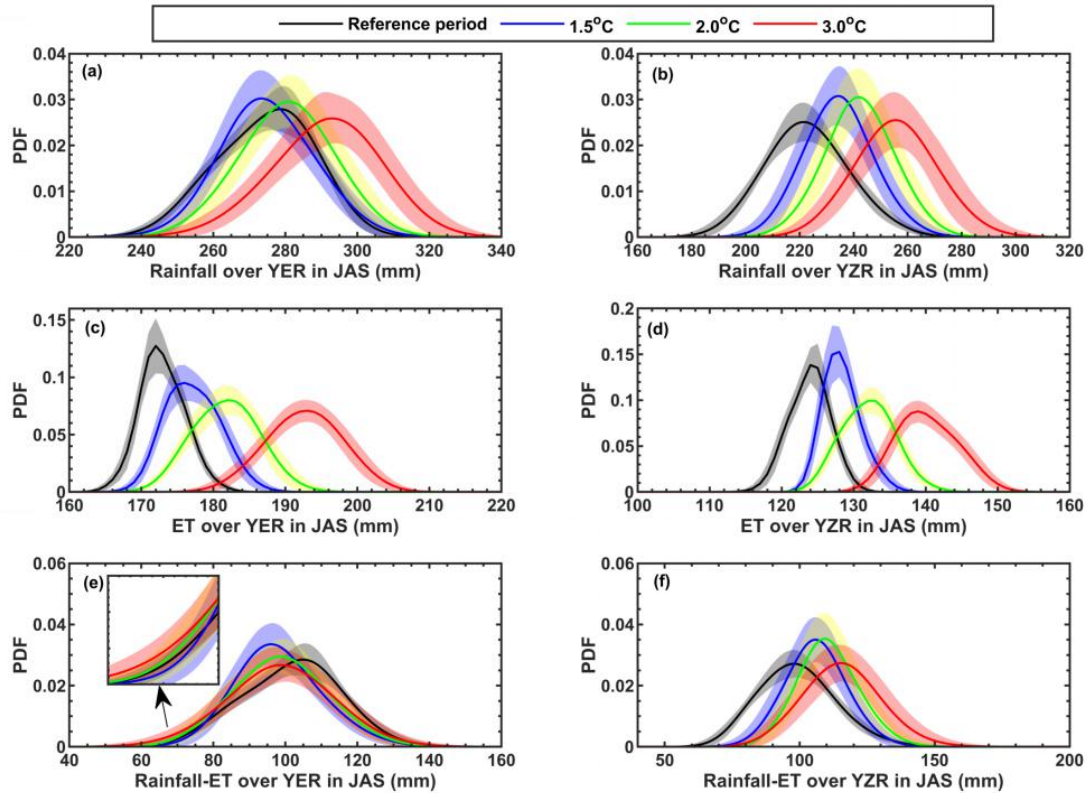


665

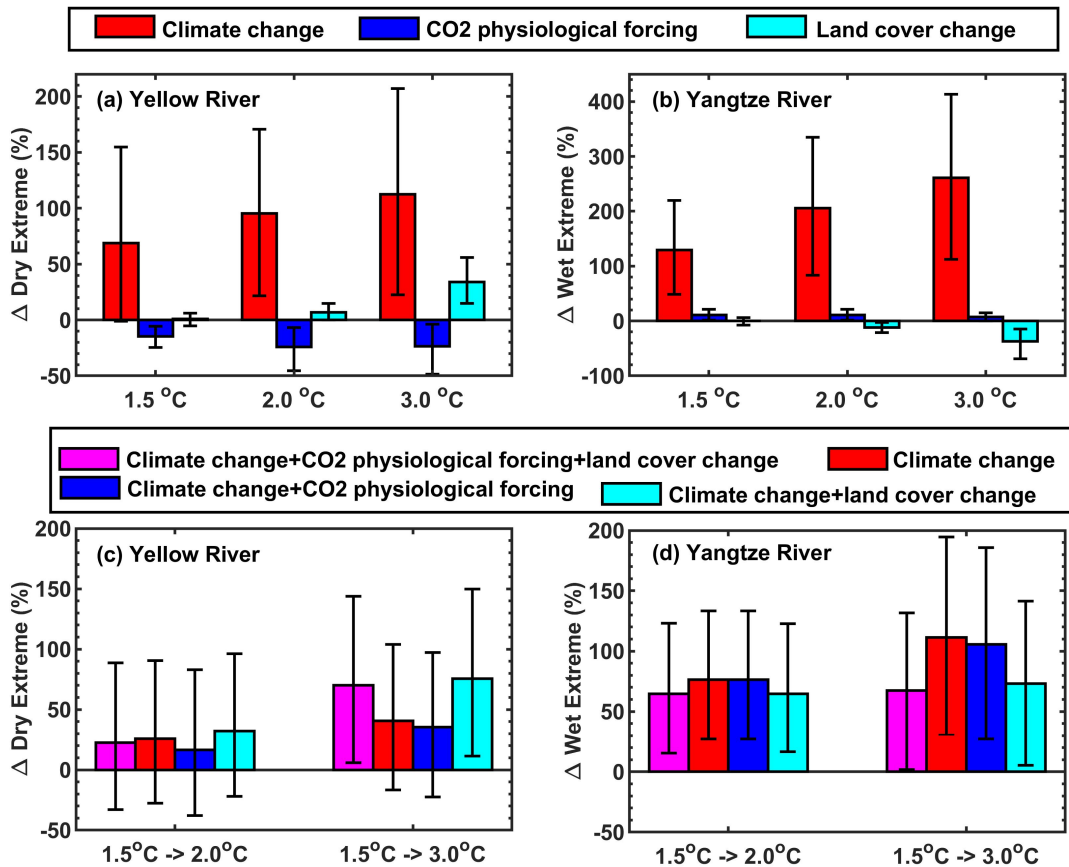
666 **Figure 34.** Box plots of relative changes of regional mean precipitation,  
 667 evapotranspiration (ET), ratio of transpiration to evapotranspiration (T/ET), total  
 668 runoff and terrestrial water storage (TWS) at different global warming levels.  
 669 Reference period is 1985-2014, and annual (ANN) and seasonal (winter: DF, spring:  
 670 MAM, summer: JJA and autumn: SON) results are all shown. Boxes show 25th to  
 671 75th ranges among 22 CMIP6\_SSP/CSSPv2 simulations, while lines in the boxes are  
 672 median values.



675 **Figure 45.** Changes of streamflow and its extremes at the outlets of the headwater  
 676 regions of the Yellow river and the Yangtze river, i.e., Tangnaihai gauge and  
 677 Zhimenda gauge. (a) Simulated monthly streamflow ~~elimatology~~ over the Yellow  
 678 river during the reference period (1985-2014) and the periods with different global  
 679 warming levels. Solid lines represent ensemble means, while shadings are ranges of  
 680 individual ensemble members. (b) Percent changes in frequency of dry and wet  
 681 extremes in July-September at different warming levels. Colored bars are ensemble  
 682 means, while error bars are 5~95% uncertainty ranges estimated by using  
 683 bootstrapping for 10,000 times. (c) and (d) are the same as (a) and (b), but for the  
 684 Yangtze river.



687 **Figure 56.** Probability density functions (PDFs) of regional mean rainfall,  
 688 evapotranspiration (ET) and their difference over the headwater regions of Yellow  
 689 river (YER) and Yangtze river (YZR) during flooding seasons (July-September) for  
 690 the reference period (1985-2014) and the periods with 1.5, 2.0 and 3.0°C global  
 691 warming levels. Shadings are 5~95% uncertainty ranges.



693

694

695

696

697

698

699

700

701

702

**Figure 67.** (a-b) Influences of climate change, CO<sub>2</sub> physiological forcing and land cover change on relative changes in frequency of the dry and wet extremes in July-September at different global warming levels for the headwater regions of Yellow river and Yangtze river. (c-d) Changes of dry and wet extremes under additional warming of  $0.5^{\circ}\text{C}$  and  $1.5^{\circ}\text{C}$  with the consideration of different factors. All the changes are relative to the reference period (1985-2014). Ensemble means are shown by colored bars while the 5~95% uncertainty ranges estimated by using bootstrapping for 10,000 times are represented by error bars.

703 **Table 1.** CMIP6 simulations used in this study. His means historical simulations  
 704 during 1979-2014 with both anthropogenic and natural forcings, SSP245 and SSP585  
 705 represent two Shared Socioeconomic Pathways during 2015-2100. Note the  
 706 CNRM-CM6-1 and CNRM-ESM2-1 do not provide r1i1p1f1 realization, so r1i1p1f2  
 707 was used instead.

No.	Models	Experiments	Realization	Horizontal Resolution
				(Longitude × Latitude Grid Points)
1	ACCESS-ESM1-5	His/SSP245/SSP585	r1i1p1f1	192×145
2	BCC-CSM2-MR	His/SSP245/SSP585	r1i1p1f1	320×160
3	CESM2	His/SSP245/SSP585	r1i1p1f1	288×192
4	CNRM-CM6-1	His/SSP245/SSP585	r1i1p1f2	256×128
5	CNRM-ESM2-1	His/SSP245/SSP585	r1i1p1f2	256×128
6	EC-Earth3-Veg	His/SSP245/SSP585	r1i1p1f1	512×256
7	FGOALS-g3	His/SSP245/SSP585	r1i1p1f1	180×80
8	GFDL-CM4	His/SSP245/SSP585	r1i1p1f1	288×180
9	INM-CM5-0	His/SSP245/SSP585	r1i1p1f1	180×120
10	MPI-ESM1-2-HR	His/SSP245/SSP585	r1i1p1f1	384×192
11	MRI-ESM2-0	His/SSP245/SSP585	r1i1p1f1	320×160

708

709 **Table 2.** Determination of “crossing years” for the periods reaching 1.5, 2 and 3°C  
 710 warming levels for different GCM and SSP combinations.

Models	1.5°C warming level		2.0°C warming level		3.0°C warming level	
	SSP245	SSP585	SSP245	SSP585	SSP245	SSP585
ACCESS-ESM1-5	2024	2023	2037	2034	2070	2052
BCC-CSM2-MR	2026	2023	2043	2034	Not found	2054
CESM2	2024	2022	2037	2032	2069	2048
CNRM-CM6-1	2032	2028	2047	2039	2075	2055
CNRM-ESM2-1	2030	2026	2049	2039	2075	2058
EC-Earth3-Veg	2028	2023	2044	2035	2072	2053
FGOALS-g3	2033	2032	2063	2046	Not found	2069
GFDL-CM4	2025	2024	2038	2036	2073	2053
INM-CM5-0	2031	2027	2059	2038	Not found	2063
MPI-ESM1-2-HR	2032	2030	2055	2044	Not found	2066
MRI-ESM2-0	2024	2021	2038	2030	2074	2051

711

712 **Table 3.** Performance for CSSPv2 model simulations driven by the observed  
 713 meteorological forcing (CMFD/CSSPv2) and the bias-corrected CMIP6 historical  
 714 simulations (CMIP6\_His/CSSPv2). The metrics include correlation coefficient (CC),  
 715 root mean squared error (RMSE), and Kling-Gupta efficiency (KGE). The KGE is  
 716 only used to evaluate streamflow.

Variables	Experiments	CC	RMSE	KGE
Monthly streamflow at TNH	CMFD/CSSPv2	0.95	165 m <sup>3</sup> /s	0.94
station	CMIP6_His/CSSPv2	0.76	342 m <sup>3</sup> /s	0.71
Monthly streamflow at ZMD	CMFD/CSSPv2	0.93	169 m <sup>3</sup> /s	0.91
station	CMIP6_His/CSSPv2	0.82	257 m <sup>3</sup> /s	0.81
Monthly terrestrial water storage anomaly over the Sanjiangyuan region	CMFD/CSSPv2	0.7	22 mm/month	-
storage anomaly over the Sanjiangyuan region	CMIP6_His/CSSPv2	0.4	24 mm/month	-
<b>Sanjiangyuan region</b>				
Annual evapotranspiration	CMFD/CSSPv2	0.87	14 mm/year	-
over the Sanjiangyuan region	CMIP6_His/CSSPv2	0.47	13 mm/year	-

717

718